2010

Influence of metal nanoparticles on fluorescence properties

Vamsi K. Kandimalla

Influence of Metal Nanoparticles on Fluorescence Properties

By

Vamsi Krishna Kandimalla

Thesis

Submitted to the Department of Chemistry

Eastern Michigan University

in partial fulfillment of the requirements

for the degree of

MASTER OF SCIENCE

in

Chemistry

November, 2010

Ypsilanti, Michigan.

DEDICATION

to

My Family, Friends, and EMU.

Acknowledgements

I would like to express my sincere gratitude to Dr. Timothy Brewer, my research advisor, for giving me the opportunity to work on this project. His encouraging guidance and constructive support throughout this project helped me to develop this project and thesis.

I would like to express my gratitude to my committee members Dr. Maria Milletti, Dr. Vance Kennedy, and the Head of the Chemistry Department, Dr. Ross Nord, for their suggestions and support in completing this thesis.

I would like to express my gratitude once again to Dr. Timothy Brewer, my academic advisor, who supported and guided me in the right direction through my stay at Eastern Michigan University (EMU).

I am grateful to Dr. KrishnaSwamy Rengan for providing the admission into EMU.

I would like to thank all my co-workers, especially Mussa M Haji-Jama and Adewunmi Adetayo, who helped me in synthesizing the silver and gold nanoparticles.

I would like to express my gratitude to all the members of the Chemistry Department and at EMU for their wonderful support during my study at EMU.

I would like to thank Chemistry Department Sellers fund and Graduate School for providing financial support throughout my stay at EMU.

Finally I would like to thank my father, Hanumaiah Kandimalla; my mother, Rajeswari Kandimalla; and both my uncles, Krishna Prasad Doppalapudi and Veeraiah Narne,

for their great love and support to fulfill my dreams.

Abstract

In this project, we studied the effect of silver and gold nanoparticles of various sizes on the fluorescence properties of tris (2, 2-bipyridyl) dichloro ruthenium (II) hexahydrate (Ru $(bpy)_3^{2+}$), tryptophan and phenylalanine. For (Ru $(bpy)_3^{2+}$) absorbed on silver and gold nanoparticles, the fluorescence intensity was quenched and showed a significant increase in the fluorescence lifetimes. These quenched intensities were due to energy transfer processes from the donor (Ru $(bpy)_3^{2+}$) to the metal nanoparticles. Conversely, tryptophan showed enhanced fluorescence intensities with an increase in the size of the nanoparticles, which may be attributed to the effect of fluorescence resonance energy transfer and the overlap of the emission band of fluorophore with surface plasmon resonance bands of metallic nanoparticles. Phenylalanine, however, showed a decrease in fluorescence intensities in the presence of gold and silver nanoparticles. Thus the observed fluorescence properties of tris (2,2-bipyridyl) dichloro ruthenium (II) hexahydrate, tryptophan, and phenylalanine on silver and gold nanoparticles may be useful for the design of new analytical tools that can be used in the fields of labeling, biosensing, and bioimaging.

Table of Contents

List of Tables

List of Figures

CHAPTER 1:

INTRODUCTION

1.1 Fluorescence:

Fluorescence is a luminescence process that occurs when an atom or molecule relaxes to its ground state, after being electrically excited, by emitting light. A molecule that is capable of fluorescing is called a fluorophore. When light from an external source interacts with the fluorophore, the fluorophore absorbs the light energy, resulting in a higher energy state. As the excited fluorophore is unstable at higher energy states, it relaxes from its higher energy state to a meta-stable state via small nonradiative transitions and then finally releases its excess energy from the meta-stable excited state to the ground state via a radiative transition through the process of emission of light. The light energy emitted by a fluorophore is always longer in wavelength than the light energy absorbed, due to some non-radiative energy loss during its transition to the ground state.

Recently fluorescence has become a primary methodology in life sciences because of its sensitivity, ease of use, and versatility. [1] It has been used as an imaging tool in clinical diagnosis and monitoring processes in biological systems. [2] The detection limit of a fluorescent substance is calculated by the ratio of signal to the background emission due to a substance's auto fluorescence. Because of this interfering background

fluorescence, studies have been performed to achieve high fluorescence yields. [3]

Fluorescent probes developed earlier with engineered biomarker functionalities could allow light to penetrate into biological membranes, offering the potential for diagnosis and imaging at depths in living tissues which lack bright fluorescent emissions.[4] The above two factors prompted the need for enhanced fluorescence to provide more precise diagnosis and better imaging capabilities.

A wide range of methods have been developed for enhanced fluorescence to increase the sensitivity of fluorescence, such as optical fiber fluorescence detectors. Of all the methodologies, metal enhanced fluorescence (MEF) has been the most widely investigated and explored. The attractive changes in fluorescent properties of fluorophores due to this MEF include increased rates of excitation, increased quantum yields, and decreased fluorescence lifetimes with an increased photostability. The presence of these metallic structures in the vicinity of the fluorophore can alter the optical properties of the fluorophore by increasing the excitation field depending on the distance between the metal nanoparticle and fluorophore.[5-6] Drexhage in 1974 explored metal-fluorophore interactions and explained that enhanced fluorescence and decreased lifetimes were due to changes in the fluorophore's radioactive decay rate. That work showed that metals in the form of nanoparticles, colloids or clusters could significantly enhance fluorescence.[7-9]

1.2 Nanotechnology:

Recently, nanotechnology has been one of the hyped areas in the fields of science and technology. Nanotechnology takes place on the scale of 1-100 nanometers.

An atom measures about 10^{-10} meters, and a nanometer represents a collection of a few atoms and molecules.[10-12] Properties of bulk substances that are larger than nanoscale are different from the properties of nanoparticles of similar atoms.[13] For example, silver metal is grayish, but colloidal silver, which is in the nanometer range, is yellow. This striking effect of nanoparticles on color has been known for a quite long time, including the gold nanoparticles on the Roman Lycurgus cup, iron oxide nanoparticles in Maya blue paint, and Michael Faraday's colloidal gold solutions. [14]

The properties of nanoparticles become dependent on their size and shape. Properties differ from individual constituents to those of the bulk due to the lack of symmetry at the interface. The percentage of surface atoms increases with decreasing particle size, leading to changes in physical and chemical properties.[15-16] The main reason for studying nanoparticles is their applications in catalysis and optical systems.[17] The ease in modifying the physical and chemical properties of nanoparticles with their size and shape made them interesting compared with organic dyes like Uniblue A, Acid blue 129, Methyl orange, and Congo red. [18-20]

The nano scale has also an interesting role in biological systems as most of the proteins are 1-10 nm in size. Biological systems are nanomaterials of desired shape and function acting as drug delivery agents, labeling agents and sensors.[21-23] Scientists can use these biological systems as models to build nanosystems in the lab that have similar properties.

1.3 Metal Enhanced Fluorescence:

Nearby conducting metallic nanoparticles can alter the free space conditions that

increase or decrease the incident electric field E_m felt by a fluorophore while increasing or decreasing the radiative decay rate.[24-25] These effects can be explained by the changes in photonic mode density, with large photonic density influencing the radiative decay rates and increasing the number of pathways available to release its excited energy.[26]

In Figure 1, a fluorophore with no metal attached has a radiative lifetime of t_o with low photonic density, and the fluorophore with metal attached to it has a lower radiative life time of t ($t < t_o$), with higher photonic mode density.[27]

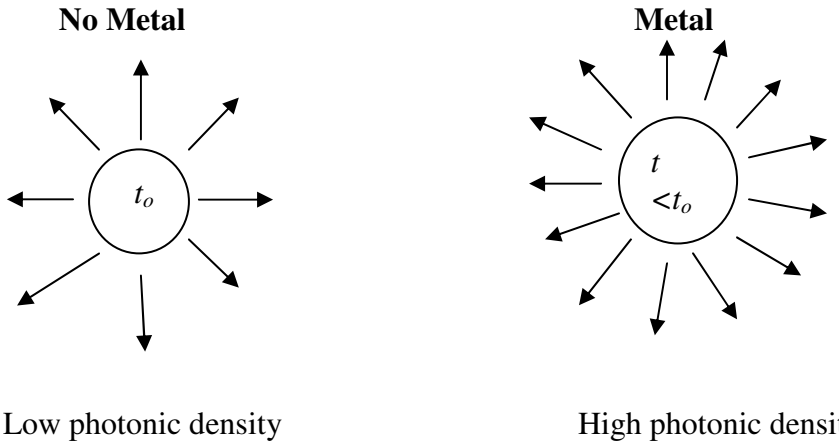

Figure 1. Low and high photonic mode densities of fluorophore in the absence and presence of metal, respectively.

When a fluorophore is electrically excited from its ground state S_o to its first excited state S_1, after a time t_o the excited fluorophore can emit a photon at a rate T or return to its ground state through either a non radiative decay process with a rate k_{nr} or a quenching process given by a rate k_q .[28]

The quantum yield Q_o of this fluorophore is shown in equation (1)

$$Q_o = \frac{T}{T + k_{nr} + k_q} \qquad (1)$$

The lifetime of the fluorophore is shown in equation (2)

$$t_o = \frac{1}{T + k_{nr} + k_q} \qquad (2)$$

When a fluorophore is placed at a suitable distance from a metallic nanoparticle, fluorophores undergo modifications to their decay rates ($T + T_m$), where T and T_m are the decay rates of fluorophore and metal nanoparticle, respectively. With an increase in the metal decay rate there is an increase in quantum yield Q_m and decrease in lifetime t_m .[28]

The quantum yield of fluorophore with metal attached is displayed by equation (3)

$$Q_m = \frac{T + T_m}{T + T_m + k_{nr} + k_q} \qquad (3)$$

The life time of fluorophore with metal attached is given by equation (4)

$$t_m = \frac{1}{T + T_m + k_{nr} + k_q} \qquad (4)$$

A Jablonski diagram shown in Figure 2 illustrates the metal enhanced fluorescence concept.[29-32]

No Metal (Free Space condition)

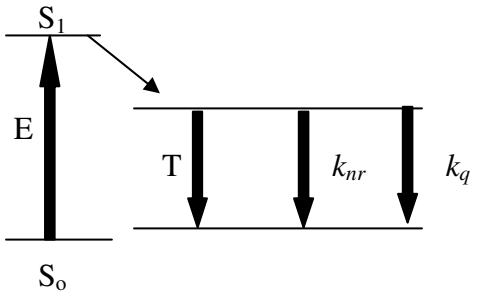

(Excitation rate E)

Metal nanoparticle

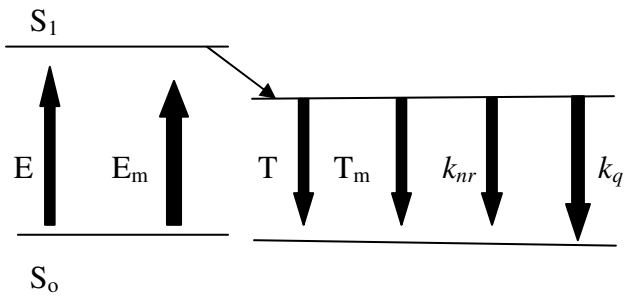

(E_m metal enhanced excitation rate)

Figure 2. Classical Jablonski diagram for the free spaced condition and the modified form in the presence of metallic particles.

The influence of metallic nanoparticle on a fluorophore is due to their close proximity to the surface and their intrinsic fluorescence property. This effect on a fluorophore by metallic nanoparticles is due to electromagnetic interactions and strong plasmon resonances at the surface which are able to produce effects like increased fluorophore photostability, increased quantum yield, increased energy transfer, and decreased lifetimes.[33-36] The size of the nanoparticles plays a role in its fluorescent properties. According to Mie theory, small particles quench fluorescence by increasing absorption, whereas larger particles enhance fluorescence by enhancing scattering.[37] When a fluorophore is within 5 nm of the surface of a metallic nanoparticle, quenching dominates over the increase in fluorescence intensity. If a fluorophore is at 10 nm or larger distance, the increase in fluorescence intensity dominates over quenching and reaches a maximum at a certain distance. At larger metal-fluorophore separations, the

enhancement of fluorescence intensity gradually decreases.[38] The presence of metallic nanoparticles near a fluorophore not only affects the lifetime and increases the quantum yield but also stabilizes adjacent fluorophores against photo bleaching by reducing the lifetime to facilitate their use in bioimaging.[39] Metallic nanoparticles show unique optical properties due to excitation of surface plasmons by light resulting in an increases in the electromagnetic field. Thus these nanoparticles, when placed near to the fluorophores, have the ability to enhance fluorescence and decrease molecular excited state lifetimes. The plasmon resonant properties of these nanoparticles can be controlled by optimizing nanoparticle topology, dimensions, and composition.[40] On the other hand, metal nanoparticles also cause quenching of the fluorescence intensity when attached to a fluorophore molecule. The quenching of intensity is mostly due to electron and energy transfer processes, which involve the surface energy transfer from dye molecules to nanoparticles. The quenching is not only caused by an increase in the non-radiative rate but also by a drastic decrease in the fluorophoric radiative rate.

.

1.4 Surface plasmon resonance in noble metal nanoparticles:

Surface plasmon resonance is responsible for the effect of metal enhanced fluorescence. The‘d’ valence electrons in noble metals are free to travel through the material as these have a longer mean free path. If the nanoparticle is smaller, there will be no scattering from the bulk. If the wavelength of light is larger than the nanoparticle size, it sets up resonance conditions. The free electrons in metals oscillate due to the resonance of light with surface plasmon oscillations.[41-42] When a beam of light passes through the electron cloud, it gets polarized to one surface and oscillates in resonance with the light frequency producing standing oscillation resonance. This is

termed as surface resonance oscillation, which leads to enhanced intensities. This resonance standing condition depends upon the size and shape of the nanoparticle and fluorophore. As the size and shape are modified, the surface area changes, which leads to changes in resonance oscillations.[43-45]

1.5 Importance of Silver and Gold nanoparticles:

Nanoparticles synthesized from gold and silver have created great interest, because of their surface Plasmon resonance. [46] The oscillation plasmon frequency for silver and gold is in the visible region with strong plasmon resonance. Silver is one of the most frequently used metals for fluorescence enhancement because of its low cost. Silver nanoparticles are best when stored in water and used within a few days after synthesis because they are prone to oxidation and deterioration after long storage times or high temperatures. Gold nanoparticles resist oxidation and have a longer shelf life than silver particles. Gold nanoparticles, though more expensive, have superior stability, uniform surfaces and high affinity for organic groups providing the possibility of biocompatible nanoparticles for bioanalysis.[47]

1.6 Synthesis of Silver and Gold nanoparticles:

Synthesis of silver and gold nanoparticles is rather easy even though the size of the nanoparticles is sensitive to the temperature and reaction time. The experiments chosen to study the influence of nanoparticles on fluorescence properties were performed by using both synthesized silver and gold nanoparticles prepared in the lab and some with gold nanoparticles of known size brought from a supplier. Sizes of the synthesized silver and

gold nanoparticles are characterized using the absorption literature values because of the lack of a scanning electron microscope to characterize the size precisely. Because of this limitation and the shorter shelf life of the synthesized nanoparticles, a known size of nanoparticles was brought from a supplier.

In this current study, silver colloids were synthesized using three methods. One is the Lee-Meisel method in which colloids were produced by the reduction of silver nitrate with sodium citrate.[49] The second one is the Creighton method in which colloids were produced by the reduction of silver nitrate with sodium borohydrate.[48] The third one is the Schneider method in which the colloids were produced by the reduction of silver nitrate with sodium borohydrate dissolved in sodium hydroxide.[50] In the Lee-Meisel method, citrate reduction of silver requires addition of reducing agent to silver nitrate during stirring. If proper care is not taken during synthesis, the colloid aggregates leading to precipitation of metal. The Schneider method uses a seed growth method developed to synthesize larger nanoparticles with controlled particle size and stability. The chemical reaction involved for the synthesis of silver nanoparticles is the reduction of silver shown below.

$$AgNO_3 + NaBH_4 \longrightarrow Ag + \tfrac{1}{2} H_2 + \tfrac{1}{2} B_2H_6 + NaNO_3 \qquad (5)$$

The gold nanoparticles can be synthesized by the reduction of $HAuCl_4$ with sodium citrate. [51]

1.7 Stability of Colloidal solutions:

Two main parameters need to be considered for an analysis of the colloidal

sample. One is the stability of the colloidal solution, and the second one is the size and shape of the colloids. Stability of the nanoparticles can be achieved by proper addition of a stabilizing agent like sodium citrate. Citrate-capped nanoparticles are negatively charged and attract positively charged particles from the solution, resulting in the formation of an electrical double layer and repulsive forces between particles, which prevents agglomeration. [52] Control of the size and shape of nanoparticles is done with the seed growth method, which offers a narrow size distribution with spherical particles and prevents nucleation. In this seed growth method, metal ions are reduced and catalyzed on the surface of preformed nanoparticles. Control over the size and shape is important because they determine the properties of the nanoparticles.[53]

In this work, the influences of silver and gold nanoparticles on the fluorescence properties of tris (2,2'-bipyridyl) dichloro ruthenium(II) hexahydrate, tryptophan, and phenylalanines were studied. The Ruthenium complex was preferred, as the pulsed laser used in this work was limited to 532 nm for lifetime measurements which is in the region of the Ruthenium complex absorption, whereas the tryptophan and phenylalanine were preferred since these are easily biodegradable when used in biosensing technologies. Our results show that when varying concentrations of these fluorophores were titrated with different sizes of silver and gold nanoparticles, they display notable differences in fluorescence intensity and in lifetime compared to when no metalis present.

1.8 Research Proposal:

This thesis project investigates time resolved and steady state fluorescent measurements of tris (2,2'-bipyridyl) dicholo ruthenium(II) hexahydrate, tryptophan, and phenylalanine in the systems of silver and gold nanoparticle colloids. The project involves the characterization of the effect of nanoparticle size on fluorescence properties of fluorophores and the properties that affect fluorescence intensity. Experiments were performed on different particle sizes of silver and gold nanoparticles titrated with different concentrations of the above mentioned fluorescence dyes to study the influence of nanoparticles on the dye's fluorescence properties, which can lead to the development of a model to fully explain the influence of metal nanoparticles on fluorescence properties.

CHAPTER 2

EXPERIMENTAL

2.1 Materials:

Silver nitrate, sodium borohydride, trisodium citrate, hydrogen tetracholoaurate (III) hydrate (99% Au), ascorbic acid, tryptophan, D-phenylalanine were purchased from Sigma. Tris (2,2-bipyridyl) dichloro ruthenium(II) hexahydrate was purchased from Aldrich. KCl was purchased from Fischer Scientific and NaOH from Kodak Laboratories. Gold nanoparticles of sizes 5 nm, 10 nm, 20 nm, 40 nm, and 80 nm were purchased from Tedd Laboratories. Deionized water from a Barnstead ultra purifier was used for preparation of all aqueous solution. All the above chemical materials were used as received without further purification.

2.2 Synthesis of Silver colloids:

Silver colloids were synthesized using three different methods.

2.2.1 Creighton Method:

In the Creighton method, silver colloids were produced by the reduction of silver nitrate with sodium borohydride. In this method, 0.00386 g of sodium borohydride ($NaBH_4$) was diluted with water to 50 mL in a volumetric flask. Before proceeding with the reaction, N_2 was bubbled through the above solution and then kept in an ice bath to prevent degradation. Next a solution was made by weighing out 0.00442 g of silver nitrate ($AgNO_3$) which was diluted with water in a 25 mL volumetric flask. The final step

was to add 12 mL of the ice cold prepared aqueous solution of $NaBH_4$ to 4 mL of the $AgNO_3$ solution with vigorous stirring. This resulted in a color change to light yellow. Stirring was continued until the reaction reached room temperature.[48]

2.2.2 Lee-Meisel Method:

This method is used to obtain larger size silver nanoparticles and involves the reduction of $AgNO_3$ with sodium citrate ($C_6H_5O_7Na_3$). In this method, 0.0425 g of $AgNO_3$ was dissolved in 50 mL of deionized water. A solution of 1 % sodium citrate was made by dissolving 0.5 g in 50 mL of deionized water. The 50 mL $AgNO_3$ solution was heated to boiling, after which varying amounts of 1% silver nitrate in amounts of 1 mL, 3 mL, and 5 mL were added to make different samples. The heating continued until the solution turned a pale yellow color, and it then was allowed to cool to room temperature.[49]

2.2.3 Schneider Method:

This seed growth method to synthesize larger silver nanoparticles involves using silver seeds. The advantages of controlled particle size and homogeneity can be achieved through this method. In this method, the seed solution was prepared by reducing of silver nitrate with a solution of sodium borohydride and sodium hydroxide. A 100 mL solution containing 0.00422 g of NaOH and 0.000378 g of $NaBH_4$ was prepared. This solution was kept in an ice bath. Then 0.01019 g of $AgNO_3$ was diluted in 100 mL of deionized water. With continuous stirring, the solution of $AgNO_3$ was added to the solution of $NaBH_4$ and NaOH until a pale yellow solution was obtained. This

solution was the silver seed solution that was used to grow larger silver nanoparticles.

A 100 mL solution containing 0.00510 g of $AgNO_3$ was prepared and labeled as solution A. Then a solution of 0.00046 g of NaOH 0.1 mL was prepared and labeled as solution B. A 100 mL solution containing 0.00153 g of NaOH and 0.005283 g of ascorbic acid was prepared and labeled as solution C. Finally, a solution of 5 mL containing 0.3727 g of KCl was prepared to stabilize the reaction. KCl should be added at an early designated time interval in order to prevent oxidation and quenching which occurs in its absence. Solution A and solution C were mixed slowly with solution B, and the contents were stirred at a constant speed. The above steps were repeated by altering the amount of silver seed solution used to prepare solution B from 0.2 mL to 2 mL and slowly mixing that with solution A and C to obtain various sizes of silver nanoparticles.[50]

2.3 Synthesis of Gold colloids:

Synthesis of gold colloids was achieved by reduction of $HAuCl_4$ with sodium citrate. 0.1699 g of $HAuCl_4$ was diluted with 100 mL of deionized water. Then 1 mL of the above 100 mL solution was diluted to 19 mL. A solution of 0.5 % sodium citrate (0.25 g in 50 mL of deionized water) was made. Next, the 19 mL of diluted $HAuCl_4$ solution was heated until it began to boil. Then varying amounts (1 mL, 2 mL and 3 mL) of 0.5 % sodium citrate solution were added. Heating continued until a pale purple color solution was achieved. The solution was removed from the heat and allowed to cool to room temperature.[51]

2.4 Instrumentation:

2.4.1 Ultraviolet-visible spectrophotometer:

All the silver and gold nanoparticles that were synthesized using the above different methods were analyzed for their maximum absorption wavelength using a UV-VIS spectrophotometer in order to characterize the size of the nanoparticles

A Perkin Elmer Lambda 20 UV-VIS spectrophotometer with hydrogen and deuterium lamps as its light source for UV and visible lights, respectively, was used to determine the absorbance of the various nanoparticles synthesized. The ratio of the intensity of the light passing through the sample to the intensity before passing through the sample is defined as transmittance (%T), from which absorbance A can be calculated.[52]

$$A = - \log (\%T/100\%) \qquad (6)$$

The parts of a UV-VIS instrument include a light source, sample holder, monochromator and detector as shown in Figure 3. In general the visible light source is a tungsten filament (300 nm-2500 nm); a deuterium lamp for ultraviolet wavelengths (190 nm-440 nm) is also used. The detectors are photodiodes used in tandem with a monochromator to allow a single wavelength of light to pass through for detection. The light from the light source is split into two beams before passing through the sample. One beam is used as a reference, and the other passes through the sample. Thus, in dual-beam spectrophotometers, the detector measures the transmittance of the sample beam relative to the reference beam. Quartz cuvettes were used as they are transparent through the UV, visible, and infrared regions.[52]

.

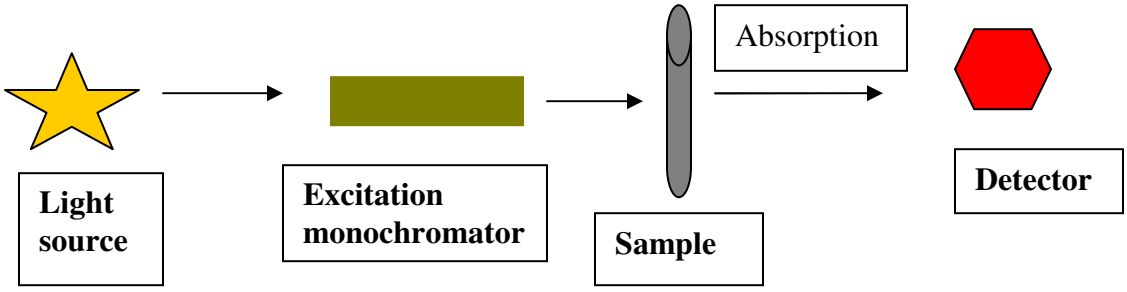

Figure 3. Schematic diagram of Absorption Spectrophotometer.

2.4.2 Spectrofluorometer :

A Spectrofluorometer measures the fluorescence of a chemical system. The parts include a light source, sample holder, excitation monochromator, emission monochromator, and detectors. Various light sources like lasers, mercury vapor lamps, and xenon arc lamps are used as the light sources to excite the molecules to their excited states. The advantage of lasers over lamps is that lasers do not need any excitation monochromators as they emit light with high irradiance at a narrow wavelength. [53] The disadvantage of lasers compared to xenon or mercury lamps is that the wavelength of the laser cannot be varied or altered. The monochromator utilizes a diffraction grating which is adjusted to select a desired wavelength for analysis.[53] Detectors used in this device are multi-channeled, which detects the intensity at all wavelengths simultaneously. The Jasco

FP-6300 spectrofluorometer used a mercury lamp as its light source and diffraction grating monochromators and photodiodes as detectors to determine the steady state fluorescent measurements. The light from a light source passes through the excitation monochromator and goes through the sample in the cuvette. This excites the electrons of the sample molecule to their excited states. Then they return to their ground states by emitting fluorescence light. This fluorescent light passes through the emission monochromator and reaches the detector, which is at 90^{o} to the incident light to reduce the risk of reflected or transmitted light reaching the detector. While measuring the fluorescence spectrum, the wavelength of the excited light is kept constant, usually at a wavelength of high absorption, and emission is observed at a single wavelength or a scan is conducted to record intensity versus wavelength. [53]

In this project, samples containing different sizes of silver and gold nanoparticle solutions that were titrated with varying concentrations of tris (2,2-bipyridyl) dichloro ruthenium(II) hexahydrate, tryptophan, and phenylalanine were analyzed using a Jasco FP-6300 for measuring the steady state fluorescence parameters.

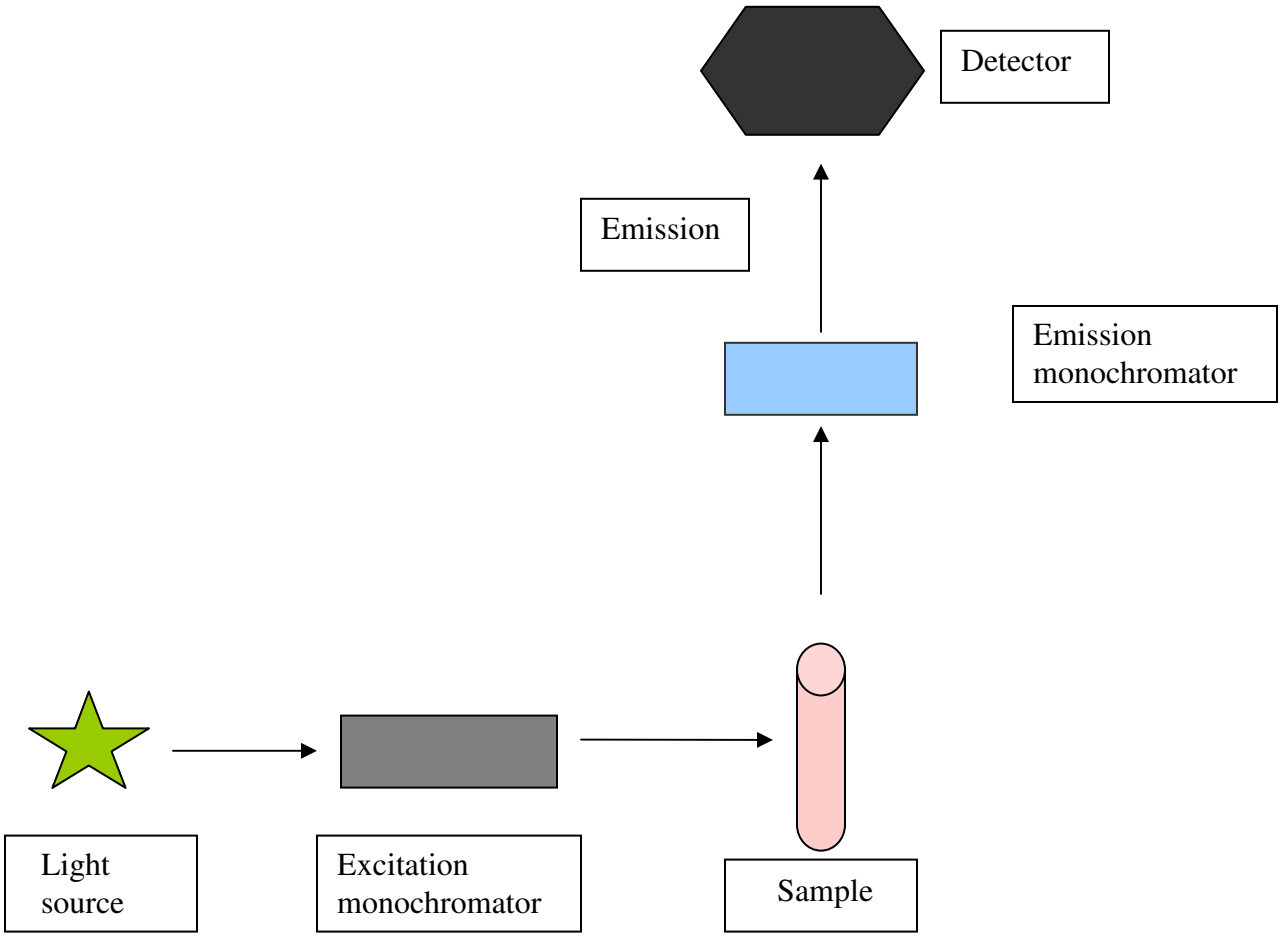

Figure 4. Schematic diagram of Spectrofluorometer

2.4.3 Pulsed Laser:

The New Wave Research Laser instrument is used to determine time resolved fluorescence, in which the fluorescence lifetime of the sample is measured as a function of time after being excited by a beam of light. This method can be used to probe the molecular environment of the nanoparticles. [54] A Pulsed laser light of 10 nanoseconds

with a wavelength of 532 nm was used to excite the fluorophores dissolved in the colloidal solution from the ground state to their excited state. The detector used in this apparatus was a Hammamatsu photomultiplier tube connected to a Hewlett-Packard 500 MHz oscilloscope which displayed the decay of the fluorescence intensity with respect to time.

In this project, fluorescence lifetimes of different samples containing different sizes of silver and gold nanoparticles were titrated with varying concentrations of tris (2, 2-bipyridyl) dichloro ruthenium(II) hexahydrate.
.

2.5 Method for preparation of Nanoparticle and fluorophore assembly:

First, synthesized silver and gold nanoparticles were analyzed to characterize their sizes using the Perkin Elmer Lambda 20 (UV-VIS spectrophotometer). Then by following a titration scheme explained later in the results, the fluorescent lifetimes and fluorescent intensities of different samples containing different sizes of silver and gold nanoparticles titrated with varying concentrations of tris (2,2-bipyridyl) dichloro ruthenium(II) hexahydrate were analyzed using a New Wave Research laser and a Jasco FP-6300 spectrofluorometer, respectively. Similar titration schemes mentioned in the results section were followed for the other fluorophores of tryptophan and phenylalanine, respectively, to study their fluorescent properties.

CHAPTER 3

RESULTS AND DISCUSSION

3.1 Size characterization of synthesized silver nanoparticles:

Silver nanoparticles were synthesized using three methods from the literature.

1) Crieghton Method
2) Lee-Meisel Method
3) Schneider Method

Absorbance spectra of the synthesized nanoparticles were used to estimate sizes from known literature absorbance values of silver nanoparticles.

Table 1. Particle size and corresponding maximum absorption wavelength of Silver nanoparticles.

Particle size /nm	Maximum absorption wavelength /nm
10	395
15	405
20	410
30	415
40	425
50	435
60	445
70	455
80	465

Table 1 shows different silver particle sizes and their respective maximum absorption wavelengths. Absorption wavelength shifts towards the red portion of the spectrum as particle size increases. Also the spectra broaden as particle size increases.[55]

3.1.1 Size characterization of silver nanoparticles synthesized using Creighton method:

Figure 5 shows the absorbance spectra of sample 1 and sample 2 of silver nanoparticles synthesized using the Creighton method. The maximum absorption wavelength of sample 1 is 407 nm and sample 2 is 405 nm. Using Table 1, these wavelengths corresponds to a particle size of about 15 nm. The reproducible absorbance peak in the spectra for two different samples shows the reproducibility of the synthesis.

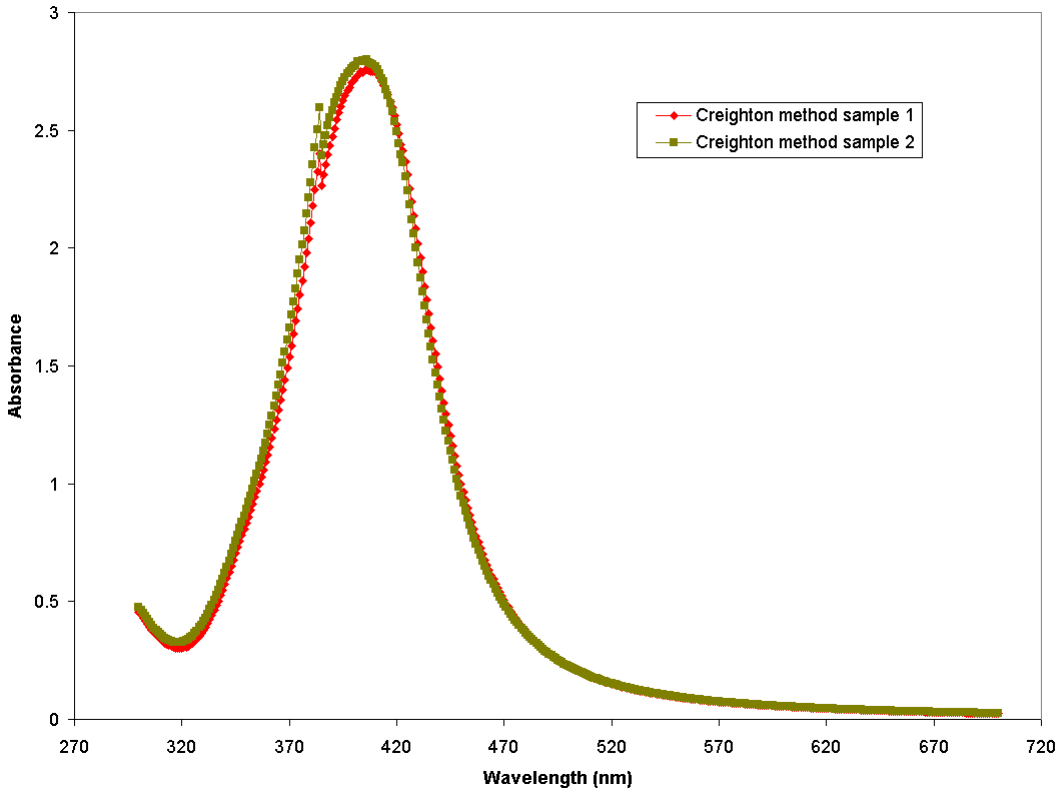

Figure 5. Absorbance spectra of silver nanoparticles synthesized using Creighton method.

3.1.2 Size characterization of silver nanoparticles synthesized using Lee-Meisel method:

Figure 6 shows the absorbance spectra of the three silver nanoparticle samples, synthesized by the reduction of 25 mL of silver nitrate with different volumes of sodium citrate (1 mL, 3mL and 5 mL). Using the maximum absorption wavelength data in Table 1, these sample sizes were estimated to be 30 nm to 40 nm for 1 mL sodium citrate, 40 nm for 3 mL sodium citrate, and 50 nm for 5 mL sodium citrate with maximum absorption wavelengths at 420 nm, 425 nm and 435 nm, respectively. The sizes of silver nanoparticles synthesized from this method are larger than those synthesized by the Creighton method.

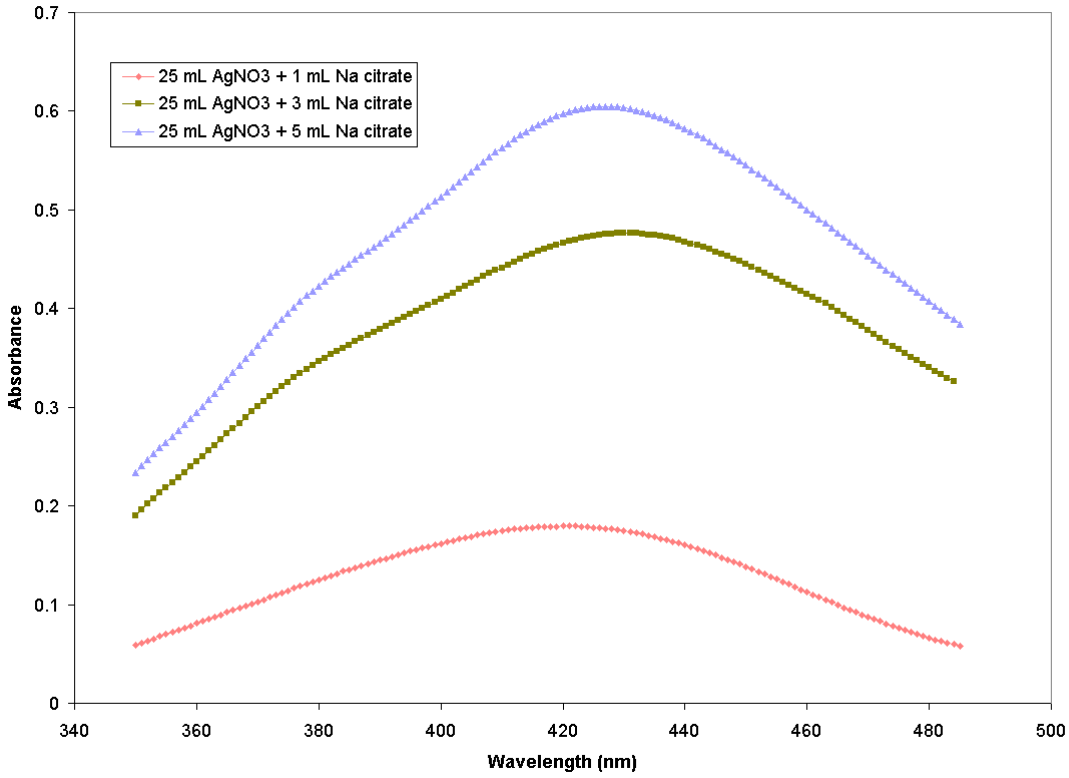

Figure 6. Absorbance spectra of silver nanoparticles synthesized using Lee-Meisel method.

3.1.3 Size characterization of silver nanoparticles synthesized using Schneider method.

Figure 7 shows the absorbance spectra of three silver nanoparticle samples synthesized using varying milliliters of silver seed solution. Using the maximum absorption wavelength data in Table 1, the sample size was estimated to be 30 nm for 0.1 mL of seed solution with its maximum absorption wavelength at 416 nm. The samples with 1 mL and 2 mL of seed solution have their maximum absorption wavelength at 465 nm and 476 nm, respectively, which corresponds to particles sizes of 80 nm and greater than 80 nm. These absorbance spectra are broader because of the larger particle sizes synthesized using this Schneider method. Using these three methods, silver nanoparticles of various sizes were synthesized, ranging from 15 nm to over 80 nm.

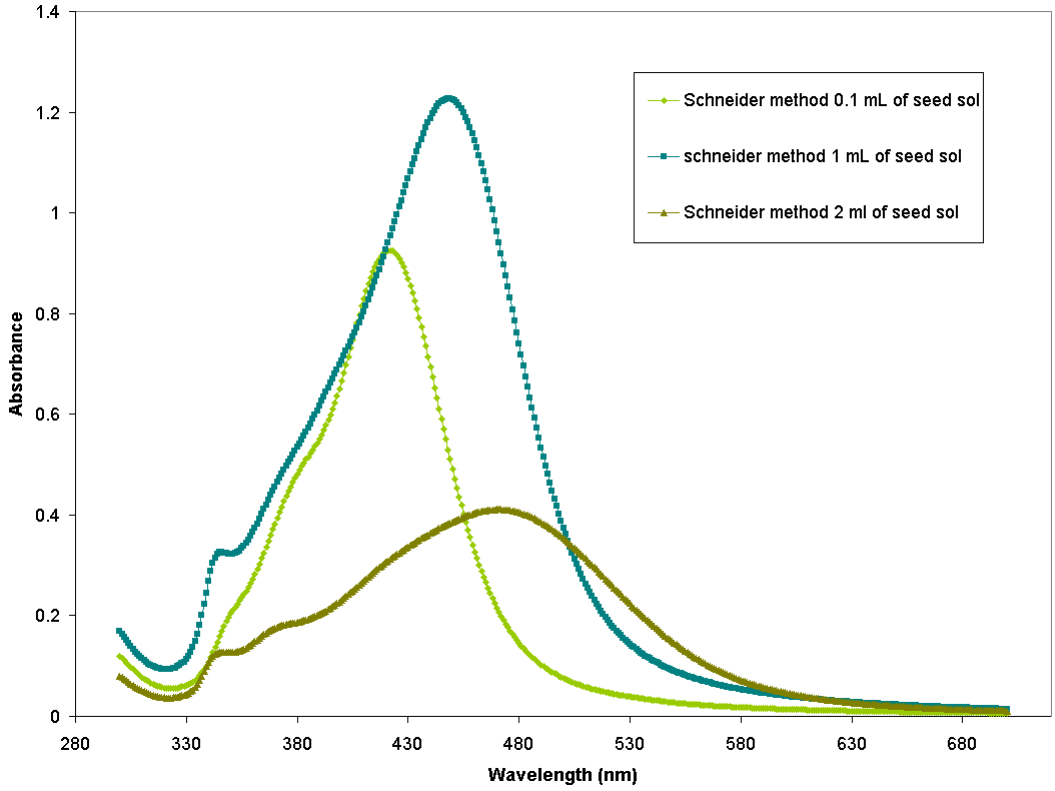

Figure 7. Absorbance spectra of silver nanoparticles synthesized using Schneider method.

3.2 Size characterization of Gold nanoparticles:

Gold nanoparticles were synthesized by the reduction of $HAuCl_4$ with sodium citrate. After synthesis, absorbance spectra of the nanoparticles were taken and the known absorbance peaks of the gold nanoparticles were used to determine the particle size of synthesized gold nanoparticles.

Table 2 shows the maximum absorbance values of different sized gold nanoparticles.[56]

Table 2. Particle size and corresponding maximum absorption wavelength of gold nanoparticles.

Particle size/ nm	Maximum absorption wavelength/nm
8-10	**518**
15	**520**
20	**526**
41	**532**
55	**534**
73	**545**

3.2.1 Size characterization of gold nanoparticles synthesized by the reduction of $HAuCl_4$ with sodium citrate.

Three samples of gold nanoparticles were synthesized using 1 mL, 2 mL, and 3 mL of 0.5 % sodium citrate. Figure 8 shows the absorbance spectra of three samples of synthesized gold nanoparticles. The sizes of all the samples were estimated using the data in Table 2. The sample with 1 mL of sodium citrate has its maximum absorption at 530 nm, corresponding to a size of 40 nm. The sample with 2 mL of sodium citrate had its

maximum absorption at 525 nm, corresponding to a size of 20 nm. The sample with 3 mL of sodium citrate had its maximum absorbance at 519 nm, corresponding to 10 nm size. An increase in the amount of sodium citrate added gradually decreased the particle size of the nanoparticle. Thus with this citrate reduction method, we were able to synthesize 10 nm, 20 nm, and 40 nm gold nanoparticles.

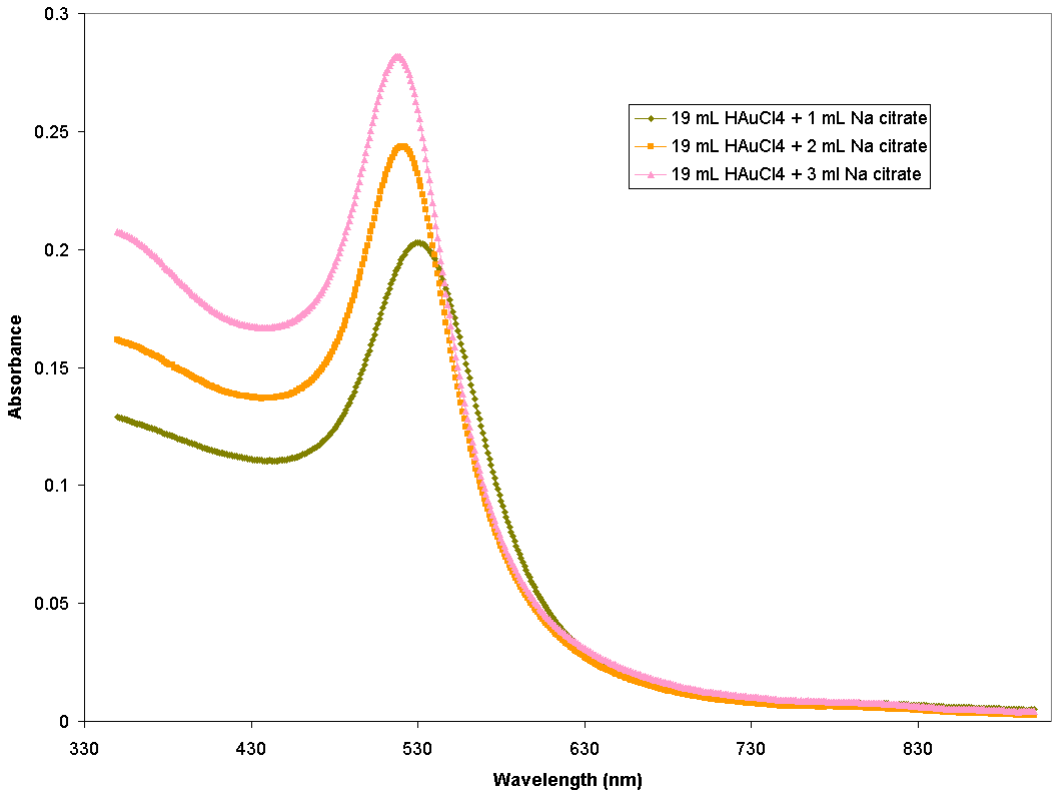

Figure 8. Absorbance spectra of gold nanoparticles synthesized by the reduction of $HAuCl_4$ with sodium citrate.

3.3 Fluorescence Spectroscopy:

Steady state fluorescence intensity measurements were taken using a

spectrofluorometer, and time resolved fluorescence measurement were taken using a 10-nanosecond pulsed laser at 532 nm. These studies were performed to show the concentration dependence of the fluorophore in the nanoparticle systems.

To prepare for the fluorescence studies, the samples containing different sizes of silver and gold nanoparticles were titrated with varying concentration of the fluorescent dyes of tris (2, 2-bipyridyl) dicholoro ruthenium (II) hexahydrate, tryptophan, and phenylalanine.

Table 3. Titration scheme for silver/gold nanoparticles with varying milliliters of 250 (uM) tris (2, 2-bipyridyl) dicholoro ruthenium (II) hexahydrate.

AgNP/AuNP (mL)	Ru complex (mL) of 250 (uM) conc	Distilled water (mL)
0.5	0.1	2.9
0.5	0.3	2.7
0.5	0.5	2.5
0.5	1.0	2.0
0.5	1.5	1.5
0.5	2.0	1.0

Table 3 shows the common titration scheme used for different sizes of silver nanoparticles (15 nm, 40 nm, 50 nm, and 80 nm) and different sizes of gold nanoparticles (5 nm, 10 nm, and 20 nm) with varying milliliters of 250 uM tris (2,2-bipyridyl) dichloro ruthenium (II) hexahydrate. AgNP and AuNP refers to silver nanoparticles and gold nanoparticles, respectively.

3.3.1 Time resolved fluorescent measurements of silver nanoparticles titrated with $Ru(bpy)_3^{2+}$:

Fluorescent lifetimes of different samples containing different sizes of silver

nanoparticles at various concentrations of ruthenium complex were analyzed using the New Wave Research Laser Doubled Nd: YAG at 532 nm with a Hammamatsu photomultiplier tube connected to a HP 500 MHz Oscilloscope.

Table 4. Fluorescence Lifetime values at 532 nm of 15 nm, 40 nm, 50 nm, and 80 nm silver nanoparticles titrated with varying concentrations of $Ru(bpy)_3^{2+}$.

[Ru] conc uM	Ruthenium complex lifetime (ns)	AgNP 15 nm + Ru complex life time (ns)	AgNP 40 nm + Ru complex life time (ns)	AgNP 50 nm + Ru complex life time (ns)	AgNP 80 nm + Ru complex life time (ns)
6.00	**437**	**451**	**445**	**449**	**490**
18.5	**420**	**433**	**437**	**439**	**466**
30.5	**392**	**426**	**422**	**436**	**445**
61.5	**310**	**311**	**372**	**396**	**439**
92.5	**320**	**300**	**355**	**374**	**397**
123	**316**	**340**	**309**	**310**	**327**

Table 4 shows fluorescence lifetime values of 15 nm, 40 nm, 50 nm, and 80 nm silver nanoparticles titrated with varying concentrations of $Ru(bpy)_3^{2+}$.

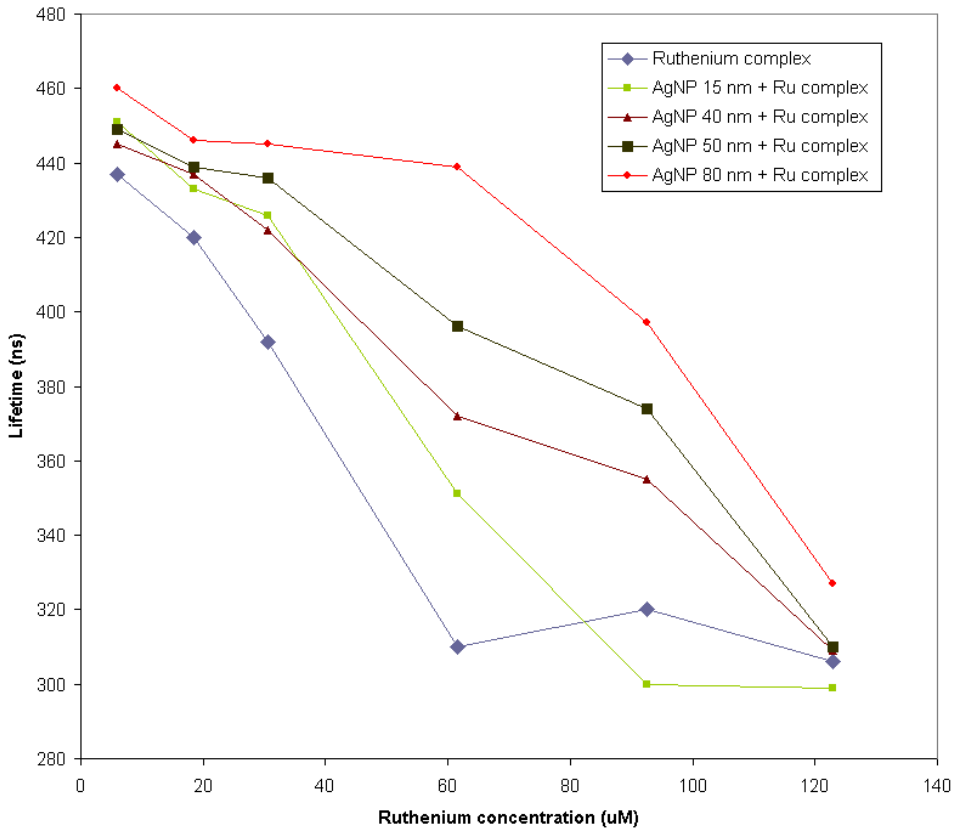

Figure 9. Fluorescence Lifetime values at 532 nm of 15 nm, 40 nm, 50 nm, and 80 nm silver nanoparticles titrated with varying concentrations of $Ru(bpy)_3^{2+}$.

Table 4 and Figure 9 show that the lifetime values for the samples containing only ruthenium complex decrease with an increase in concentration from 6.00 to 61.5 uM and then level off for larger concentrations of the complex. The lifetime values for the samples containing both the silver nanoparticles and ruthenium complex increase with an increase in size of the silver nanoparticles at constant dye concentration. On the other hand, the increase in lifetime of the samples containing the silver nanoparticles in 6.00 uM, 18.5 uM, 30.5 uM, and 123 uM ruthenium complex was only minimal, whereas the samples containing the silver nanoparticles in 61.5 uM and 92.5 uM ruthenium show a significant increase in their lifetime values. These longer lifetimes are due to the

interactions of the fluorophore with nanoparticles. The actual increase in lifetime is proposed to be due to metal fluorophore interactions and surface energy transfer. Quenching decreases the lifetime and can be more of a factor than the enhancement for certain sizes and concentrations.

3.3.2 Steady state fluorescence measurements of silver nanoparticles titrated with $Ru(bpy)_3^{2+}$:

The fluorescence intensities of samples containing different sizes of silver nanoparticles at various concentrations of ruthenium complex were analyzed using the spectrofluorometer by exciting the samples at 450 nm and recording the emission spectra from 470 nm to 700 nm.

Table 5. Fluorescence Intensities of 15 nm, 40 nm, 50 nm, and 80 nm silver nanoparticles dependence on $Ru(bpy)_3^2$.

[Ru] conc uM	Ruthenium complex Flu. intensity	AgNP 15 nm + Ru complex Flu. intensity	AgNP 40 nm + Ru complex Flu. intensity	AgNP 50 nm + Ru complex Flu. intensity	AgNP 80 nm + Ru complex Flu. intensity
6.00	0.020	0.015	0.020	0.018	0.00
18.5	0.025	0.060	0.025	0.035	0.010
30.5	0.075	0.080	0.065	0.065	0.030
61.5	0.18	0.15	0.18	0.19	0.14
92.5	0.28	0.20	0.27	0.28	0.23
123	0.35	0.28	0.33	0.33	0.30

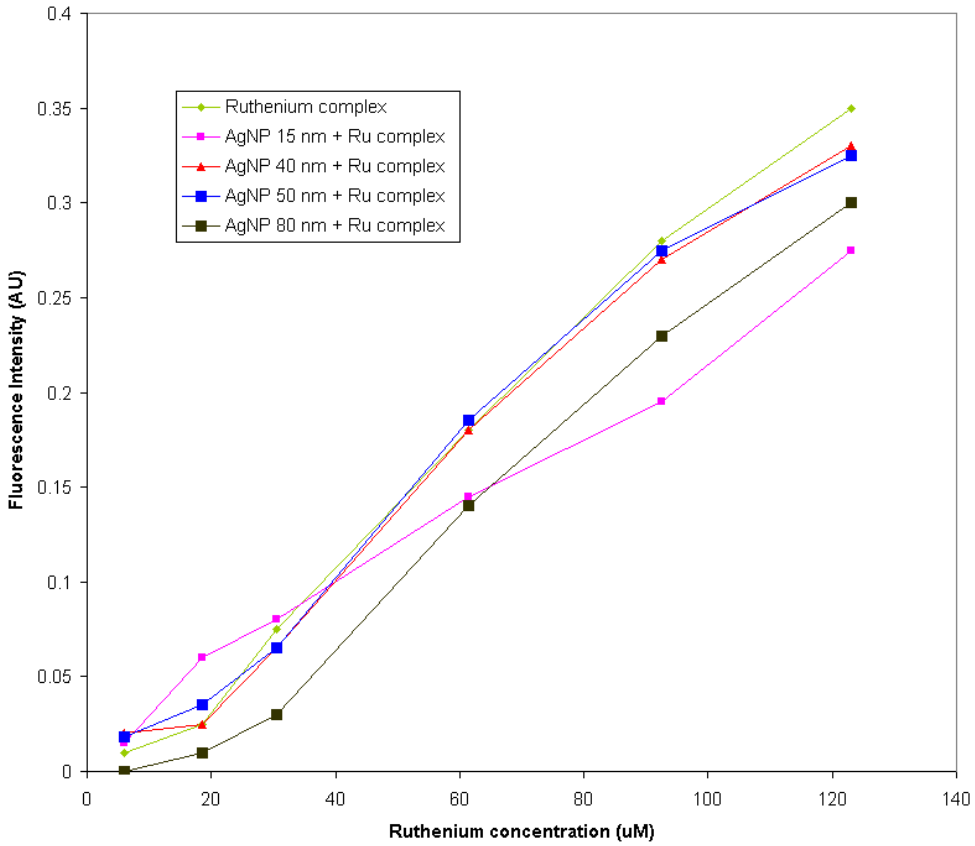

Figure 10. Fluorescence Intensities of 15 nm, 40 nm, 50 nm, and 80 nm silver nanoparticles of 0.5 mL titrated with varying concentrations of $Ru(bpy)_3^2$.

Table 5 and Figure 10 shows the fluorescence intensities of different sizes of silver nanoparticles with varying concentrations of ruthenium complex. From the above results, it was observed that binding of silver nanoparticles to the ruthenium complex quenched the intensity of ruthenium complex. The lowered intensities show that silver nanoparticles are responsible for this quenching effect. With an increase in the ruthenium concentration, the smaller silver nanoparticles of 15 nm showed greatest quenching, while the larger nanoparticles like 40 nm, 50 nm, and 80 nm quenched to a lesser extent. This quenching in the fluorescence intensity is mainly due to energy transfer from the ruthenium complex to the silver nanoparticles. When the donor molecules, like the ruthenium

complex, are in close vicinity of the acceptors, like conductive silver nanoparticles, resonance energy transfer occurs resulting in reduced fluorescence intensity.[56]

3.3.3 Time resolved fluorescent measurements of gold nanoparticles titrated with $Ru(bpy)_3^{2+}$:

Lifetime values of the samples containing different sizes of gold nanoparticles titrated with varying concentrations of ruthenium complex were analyzed using a New Wave Research Laser Doubled Nd:YAG at 532 nm with a Hammamatsu photomultiplier tube connected to a HP 500 MHz Oscilloscope.

Table 6. Fluorescence lifetime values of 5 nm, 10 nm, and 20 nm gold nanoparticles of 0.5 mL titrated with varying concentrations of $Ru(bpy)_3^2$.

[Ru] conc uM	Ruthenium complex Lifetime (ns)	AuNP 5 nm + Ru complex Lifetime (ns)	AuNP 10 nm + Ru complex Lifetime (ns)	AuNP 20 nm + Ru complex Lifetime (ns)
6.00	437	460	447	480
18.5	420	432	441	458
30.5	392	412	426	429
61.5	310	386	463	403
92.5	320	345	390	384
123	376	350	374	355

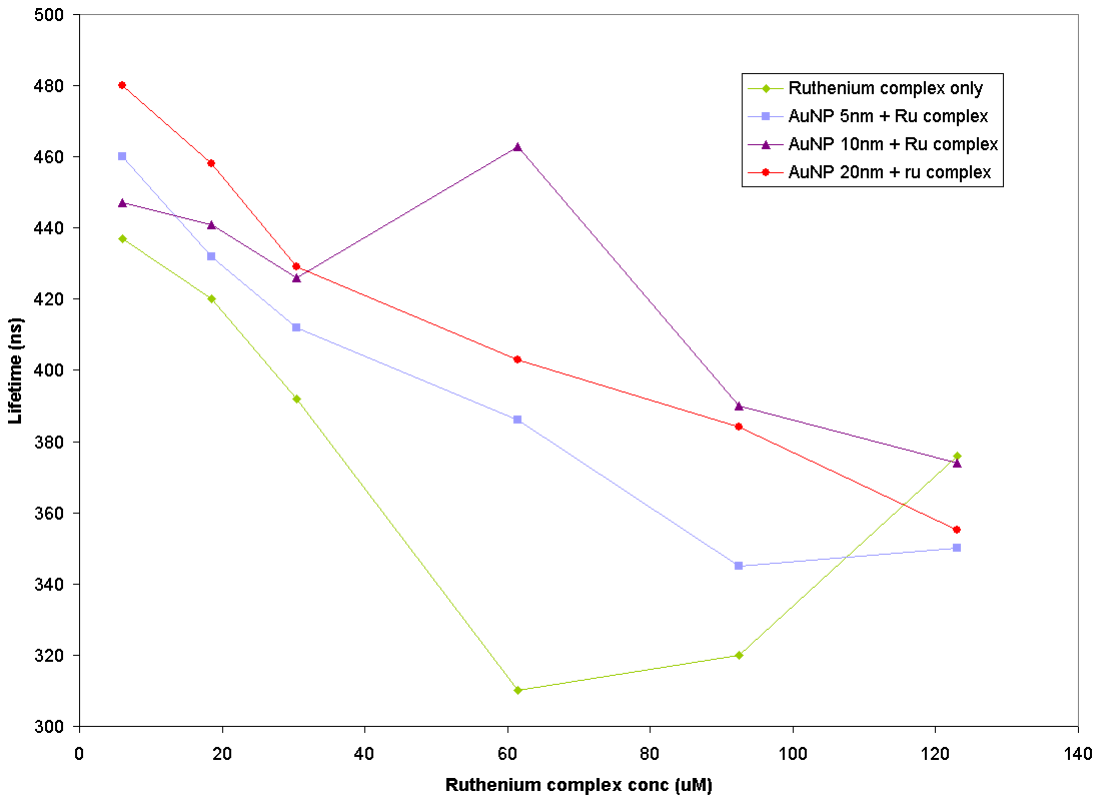

Figure 11. Fluorescence lifetime values of 5 nm, 10 nm, and 20 nm gold nanoparticles dependence on $Ru(bpy)_3^{2}$ concentration.

Table 6 and Figure 11 show the lifetime values of different samples of gold nanoparticles that were titrated with varying milliliters of 250 uM ruthenium complex. Similar to the silver nanoparticles systems, the lifetime values for the samples containing only ruthenium complex decrease with an increase in the concentrations from 6 to 61.5 uM and then level off for larger concentrations of the complex. The lifetime values for the samples containing both the gold nanoparticles and the ruthenium complex increase with an increase in the size of gold nanoparticles at constant dye concentration. Though the increase in lifetime of the samples with nanoparticles in ruthenium complex was only

slight, the lifetimes were higher than the samples with no gold nanoparticles. Thus addition of nanoparticles to the dye increased the lifetime values. The order of lifetimes is Ru < (AuNP 5 nm + Ru) < (AuNP 10 nm + Ru) ~ (AuNP 20 nm + Ru). This increase in lifetime is proposed to be due to surface energy transfer from the ruthenium complex to the gold nanoparticles.

3.3.4 Steady state fluorescence measurements of gold nanoparticles titrated with $Ru(bpy)_3^{2+}$:

Fluorescence intensities of samples containing different sizes of gold nanoparticles titrated with varying milliliters of 250 uM ruthenium complex were analyzed using a spectrofluorometer by exciting the samples at 450 nm and recording the emission spectra from 470 nm to 700 nm.

Table 7. Fluorescence intensities of the 5 nm, 10 nm and 20 nm gold nanoparticles with varying concentrations of $Ru(bpy)_3^{2+}$.

[Ru] conc uM	Ruthenium complex Flu.intensity	AuNP 5 nm + Ru complex Flu.intensity	AuNP 10 nm + Ru complex Flu.intensity	AuNP 20 nm + Ru complex Flu.intensity
6.00	0.020	0.010	0.060	0.040
18.5	0.025	0.021	0.082	0.080
30.5	0.075	0.091	0.12	0.11
61.5	0.18	0.14	0.13	0.13
92.5	0.28	0.16	0.15	0.18
123	0.35	0.19	0.19	0.22

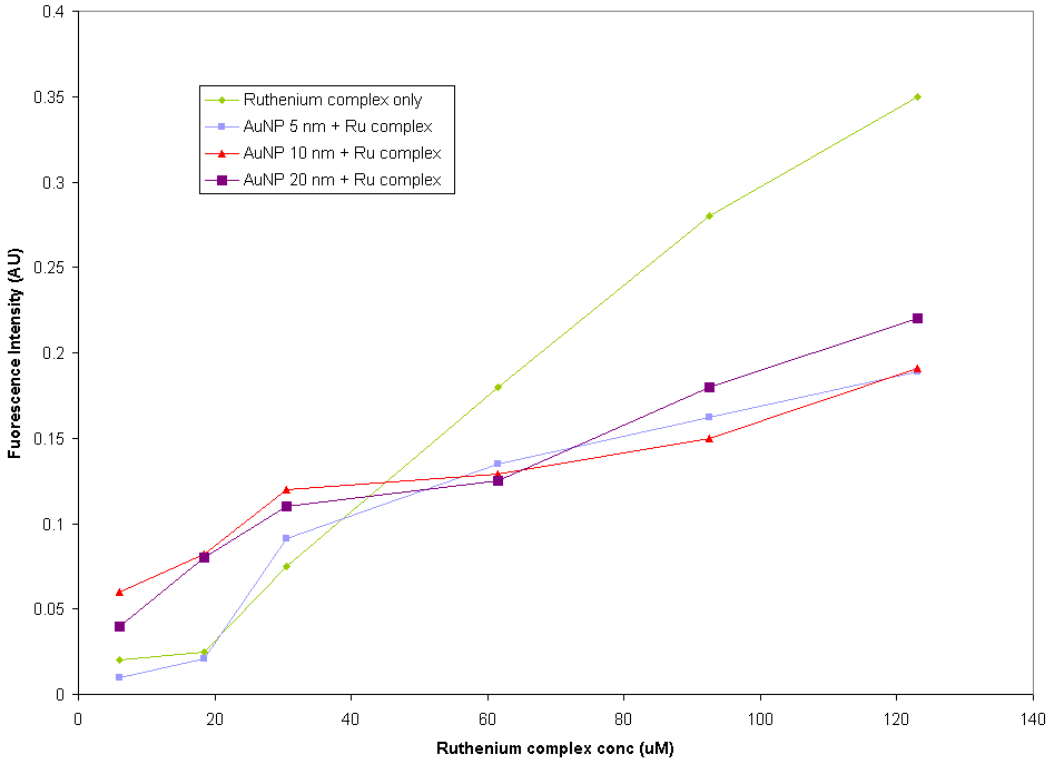

Figure 12. Fluorescence intensities of the 5 nm, 10 nm, and 20 nm gold nanoparticles titrated with varying concentrations of $Ru(bpy)_3^{2+}$.

Table 7 and Figure 12 show the fluorescence intensities of differently sized gold nanoparticles titrated with varying ruthenium complex concentrations. The intensities of samples with ruthenium complex increase with an increase in its concentration. At lower concentrations with larger gold nanoparticle size, the fluorescence intensity was enhanced, but at higher concentrations the smaller gold nanoparticles of 5 nm and 10 nm quenched the intensity slightly more than the 20 nm particles. With a decrease in gold nanoparticle size, there is an increase in the relative amount of surface area and surface atoms. This increased amount of surface area available can accommodate a larger number of ruthenium molecules around the gold nanoparticles, causing smaller particles to become more efficient quenchers than larger

particles.[56]

3.4 Steady state fluorescence measurements of samples containing different sizes of silver/gold nanoparticles titrated with varying concentrations of tryptophan.

Fluorescent intensities of samples containing different sizes of silver/gold nanoparticles that were titrated with varying milliliters of 134 uM tryptophan were analyzed using a spectrofluorometer exciting at 280 nm and recording the emission spectra ranging from 300-500 nm .

Table 8 shows the scheme used for titration of silver and gold nanoparticles with tryptophan.

Table 8. Titration scheme for silver/gold nanoparticles with varying concentrations of tryptophan.

AgNP/AuNP (mL)	Tryptophan (mL) of 134 (uM) of conc	Distilled water (mL)
0.5	0.0	3.0
0.5	0.1	2.9
0.5	0.3	2.7
0.5	0.5	2.5
0.5	1.0	2.0
0.5	1.5	1.5
0.5	2.0	1.0

3.4.1 Steady state fluorescent measurements of samples containing 15 nm, 40 nm, 50 nm and 80 nm sizes of silver nanoparticles titrated with varying concentrations of tryptophan.

Different sizes of silver nanoparticles were titrated with various concentrations of tryptophan, and the measured intensities are plotted as a function of wavelength in

Figures 13 to 17.

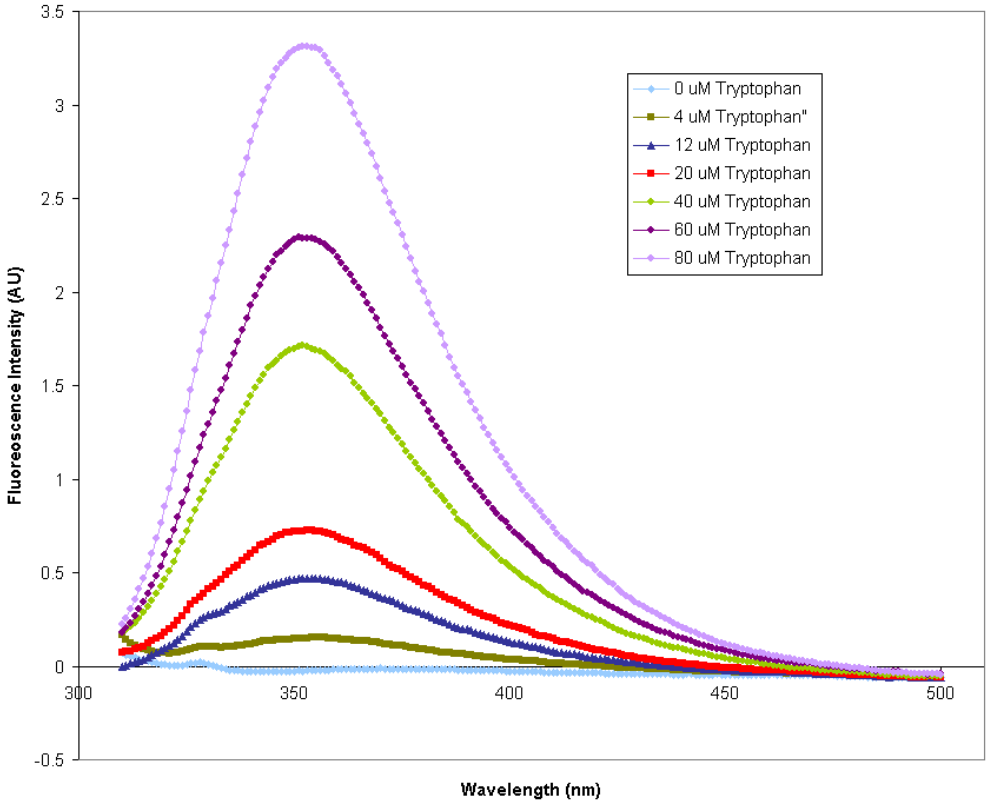

Figure 13. Fluorescence spectra of the samples containing various concentrations of tryptophan.

Figure 13 shows a gradual increase in the fluorescence intensity with an increase in tryptophan concentration that obeys Beers law as intensity increases linearly with concentration.

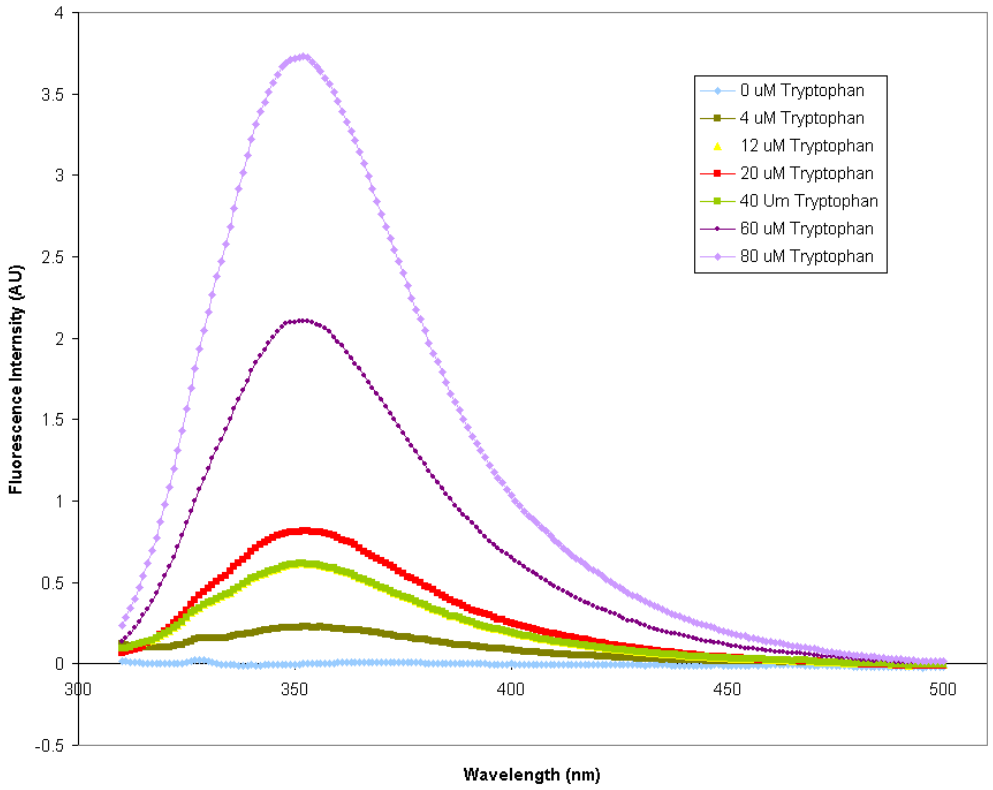

Figure 14. Fluorescence spectra of 15 nm silver nanoparticles titrated with various concentrations tryptophan.

Figure 14 shows the intensity of the samples containing 15 nm silver nanoparticles titrated with various tryptophan concentration. These samples with nanoparticles in the tryptophan had higher intensity values than samples with only tryptophan. Thus, addition of 15 nm silver nanoparticle to the dye enhanced the fluorescence intensity.

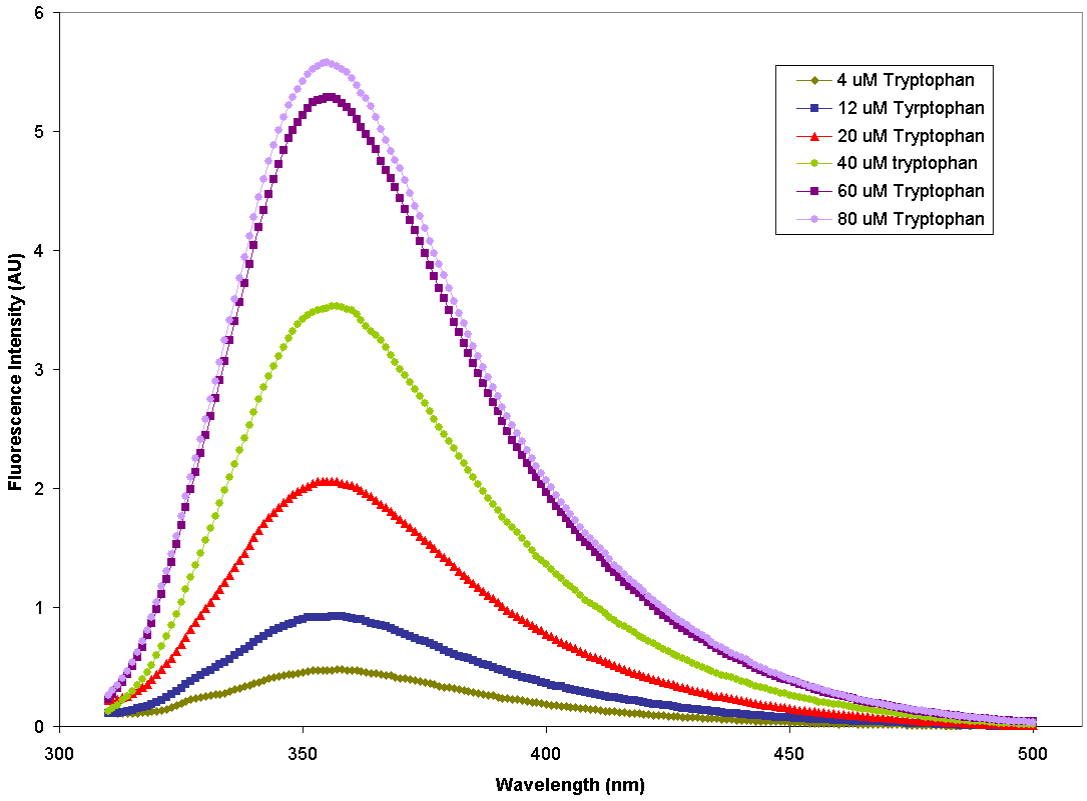

Figure 15. Fluorescence spectra of 40 nm silver particles titrated with various concentration of tryptophan.

When compared with Figure 14, Figure 15 shows that the samples containing 40 nm silver nanoparticles with tryptophan have more enhancement of their intensities than 15 nm silver particle samples with tryptophan. This increase in intensity was especially seen with particle sizes from 15 nm to 40 nm.

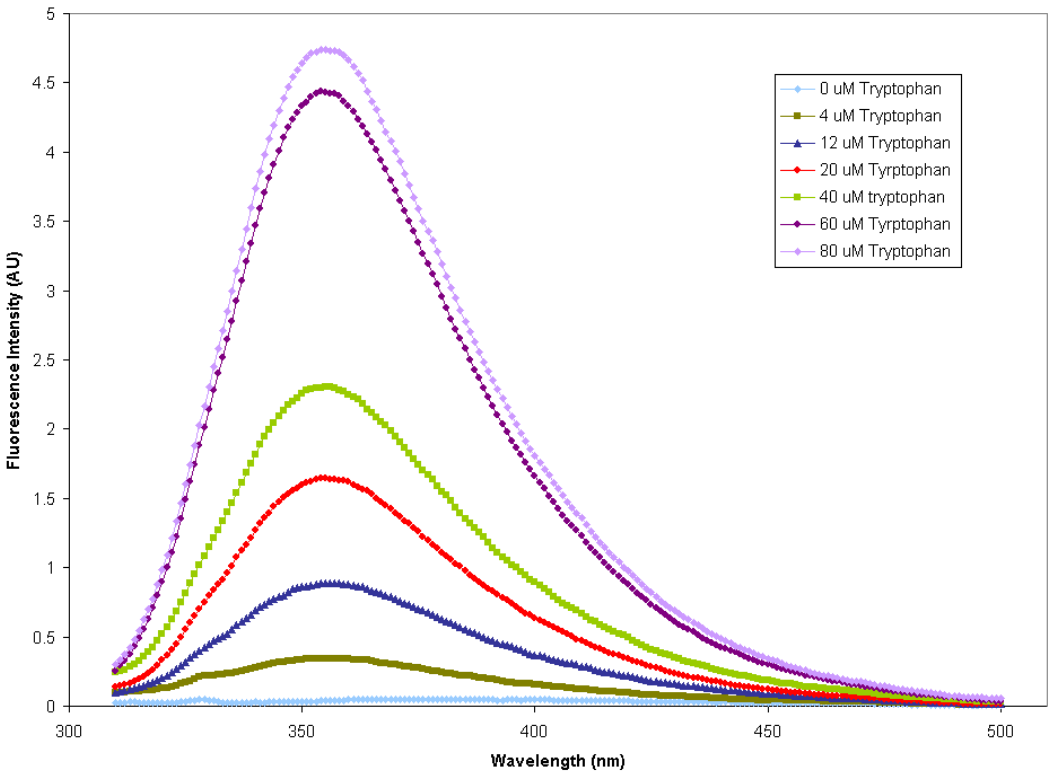

Figure 16. Fluorescence spectra of 50 nm silver particles titrated with various concentration of tryptophan.

Figure 16 shows the intensity of the samples containing 50 nm silver nanoparticles titrated with various concentrations of tryptophan. The intensities of these 50 nm silver nanoparticle samples were less than the 40 nm samples.

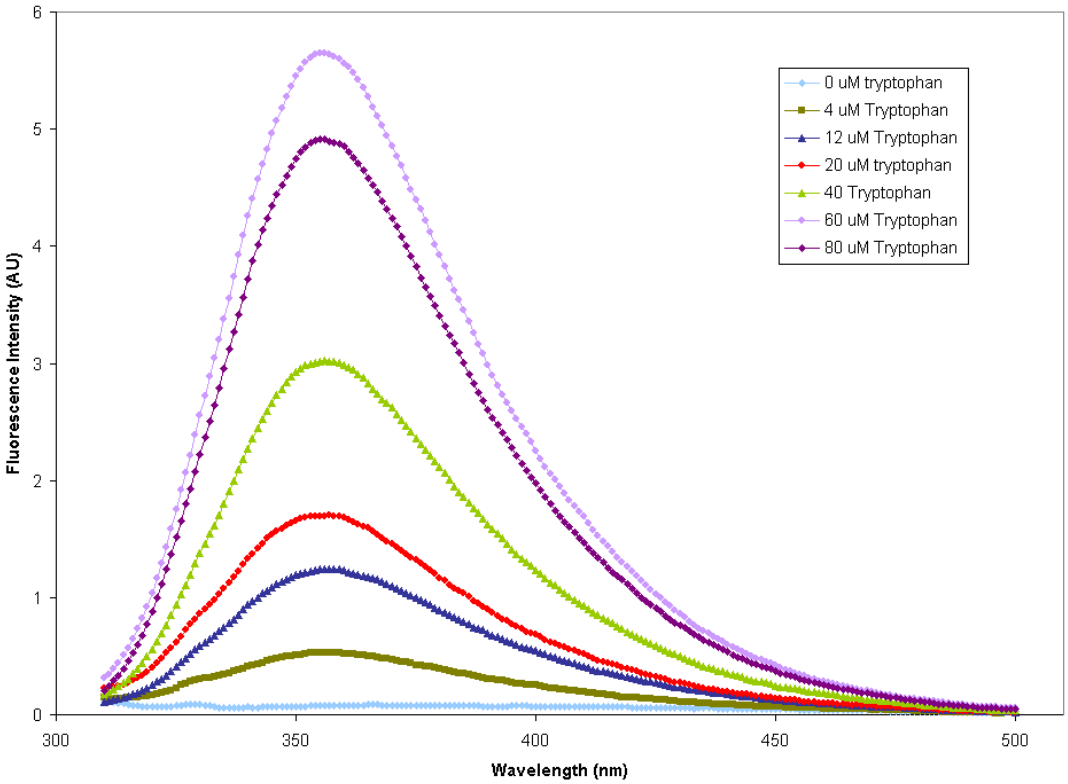

Figure 17. Fluorescence spectra of 80 nm silver particles titrated with various concentration of tryptophan.

Figure 17 shows an increase in the intensity values of the samples containing 80 nm silver nanoparticles with varying concentrations of tryptophan, when compared to the intensity of the samples with smaller nanoparticles.

Table 9. Fluorescence intensity values of samples at 350 nm containing 15 nm, 40 nm,50 nm and 80 nm sizes of silver nanoparticles titrated with varying concentrations of tryptophan.

Tryptophan conc (uM)	Tyrptophan Flu.intensity	AgNP 15 nm+Tryptophan Flu.intensity	AgNP 40 nm+Tryptophan Flu.intensity	AgNP 50 nm+Tryptophan Flu.intensity	AgNP 80 nm+Tryptophan Flu.intensity
0.00	0.070	0.010	0.030	0.052	0.13
4.00	0.17	0.22	0.47	0.34	0.54
12.0	0.46	0.61	0.92	0.90	1.2
20.0	0.72	0.82	2.1	1.7	1.8
40.0	1.7	0.63	3.5	2.4	3.0
60.0	2.3	2.1	5.3	4.5	5.7
80.0	3.4	3.7	5.6	4.7	5.0

Table 9 displays the fluorescence intensity for 0 uM of tryptophan which should be 0 at the baseline, but the small correction is due to a small amount of silver nanoparticle fluorescence.

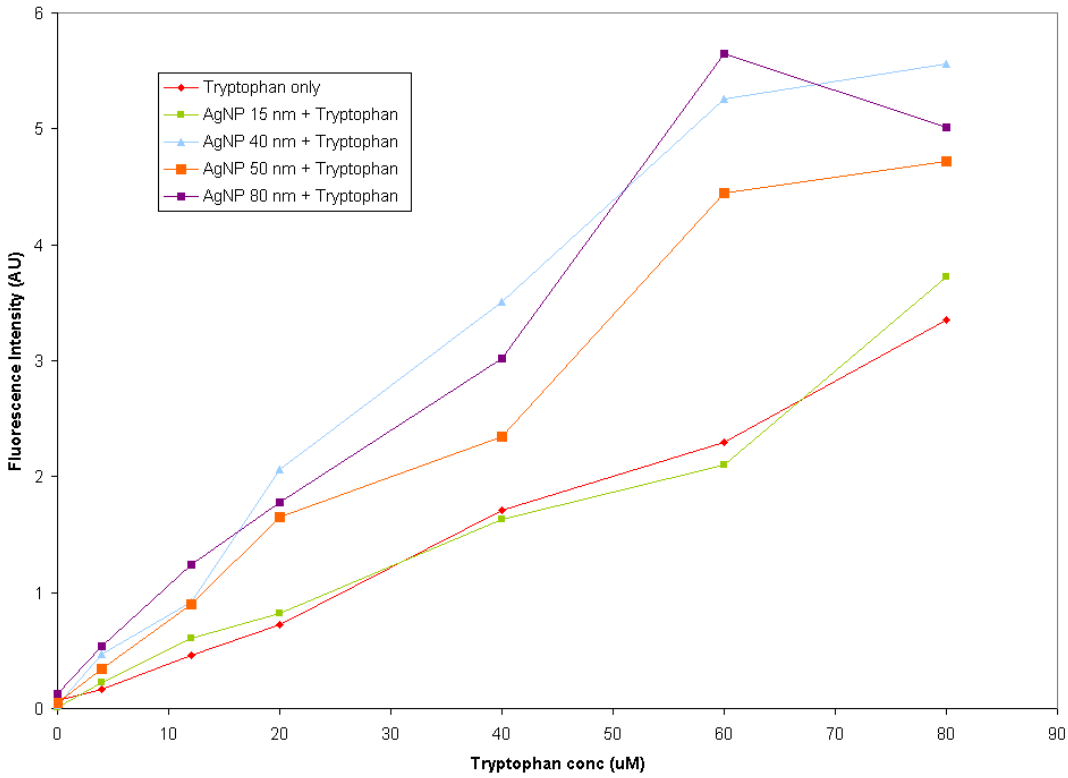

Figure 18. Fluorescence intensity values of samples containing 15 nm, 40 nm,50 nm and 80 nm sizes of silver nanoparticles titrated with varying concentrations of tryptophan at 350 nm

Table 9 and Figure 18 show a gradual increase in intensity of the samples with an increase in both tryptophan concentration and particle size of the silver nanoparticles. The addition of nanoparticles to the tryptophan solution enhanced the intensity. The sample having the highest tryptophan concentration of 80 uM and largest particle size of 80 nm have the highest intensity of all the samples. The 15 nm silver nanoparticles with tryptophan showed the least enhancement. This increase in fluorescence intensity is due to the enhancement effect of the incoming and outgoing electric fields via coupling to the surface plasmon resonance of silver nanoparticles and resonance energy transfer. This observed enhancement in emission intensity from tryptophan can be attributed to electromagnetic field enhancement of the silver nanoparticles, which was induced by the excited surface plasmons in the silver nanoparticles.[57]

3.4.2 Steady state fluorescence measurements of samples containing 10 nm, 20 nm, 40 nm and 80 nm sizes of gold nanoparticles titrated with varying concentrations of tryptophan.

Different sizes of gold nanoparticles were titrated with various concentrations of tryptophan and the fluorescence intensities as a function of wavelength are plotted in Figures 19 to 23.

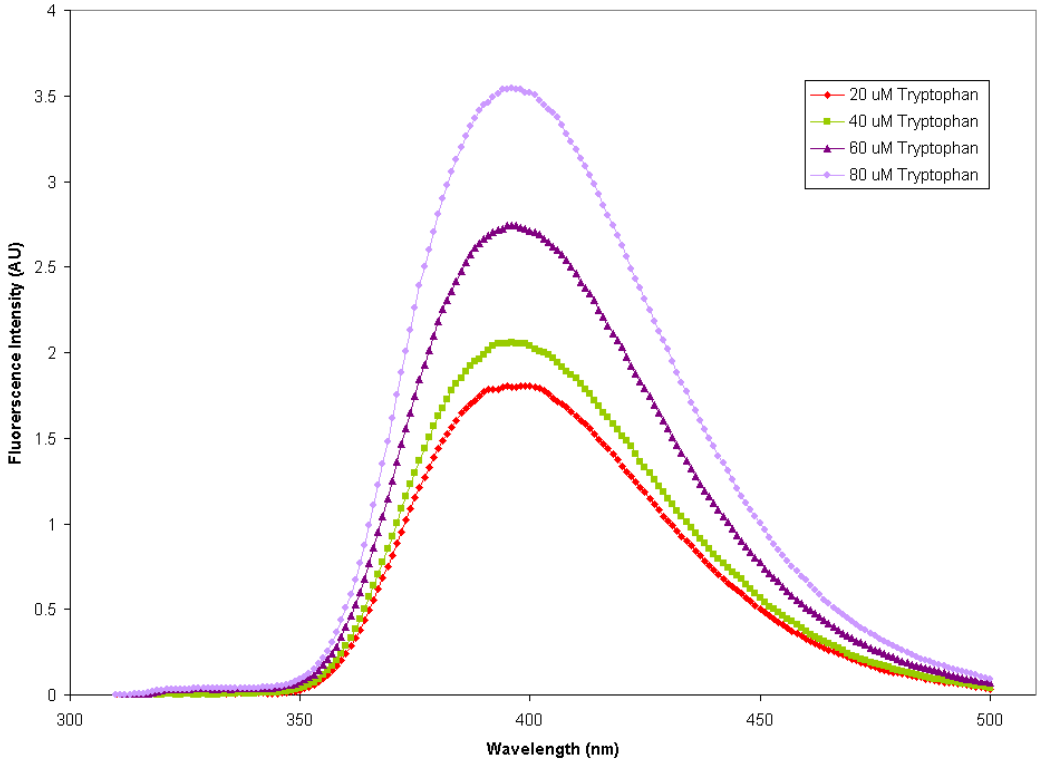

Figure 19. Fluorescence spectra of 10 nm gold nanoparticles titrated with various concentrations of tryptophan.

Figure 19 shows increased fluorescence intensity of the samples containing 10 nm gold nanoparticles with varying concentrations of tryptophan. This analysis showed that addition of 10 nm gold nanoparticles to tryptophan enhanced the intensity when compared to samples with only tryptophan.

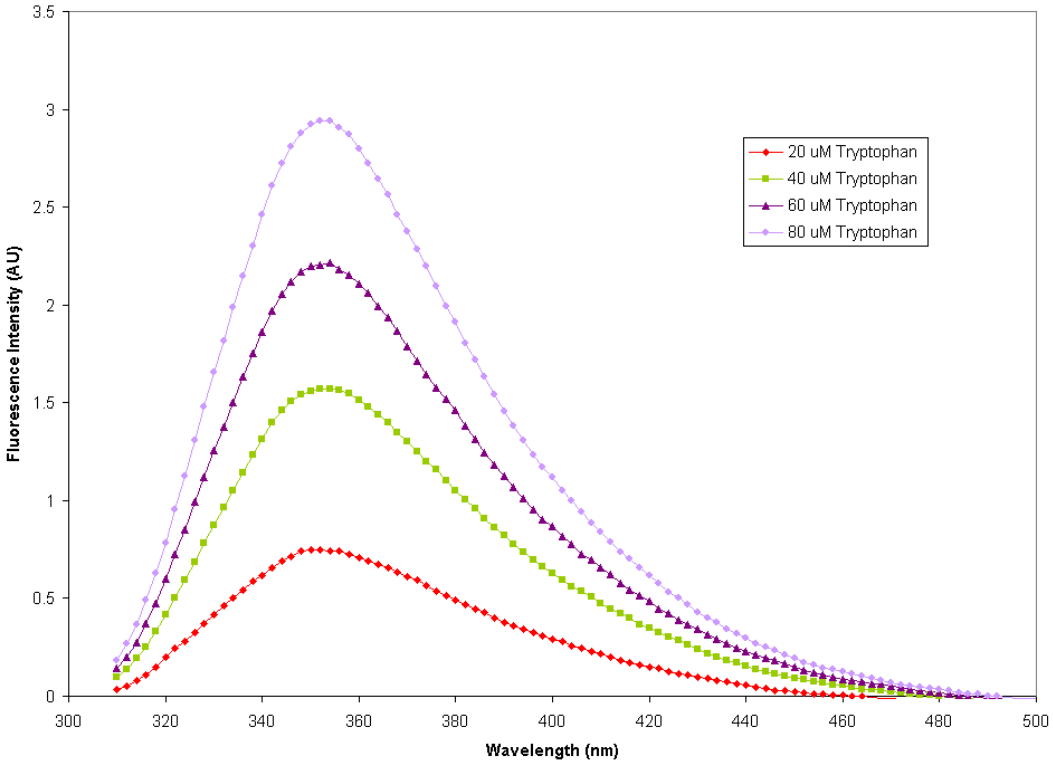

Figure 20. Fluorescence spectra of 20 nm gold nanoparticles titrated with various concentrations of tryptophan.

Figure 20 shows an increase in the intensity of samples containing 20 nm gold nanoparticles with increased tryptophan concentration. But the intensities of these 20 nm gold particle samples showed decreased intensities compared with tryptophan-only samples and 10 nm gold nanoparticle samples.

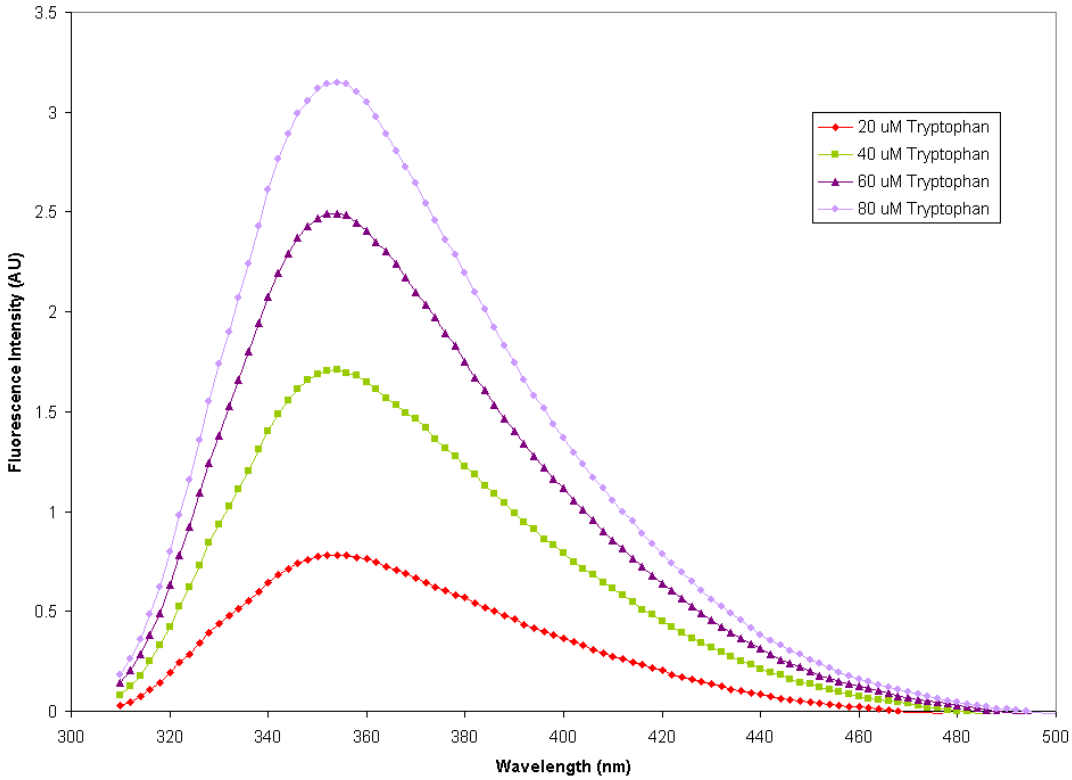

Figure 21. Fluorescence spectra of 40 nm gold nanoparticles titrated with various concentrations of tryptophan.

Figure 21 shows increased in intensity of samples containing 40 nm gold nanoparticles with various concentrations of tryptophan. The intensities of these samples are higher than only tryptophan and 20 nm gold nanoparticles samples but lower than the intensities of 10 nm gold nanoparticles samples.

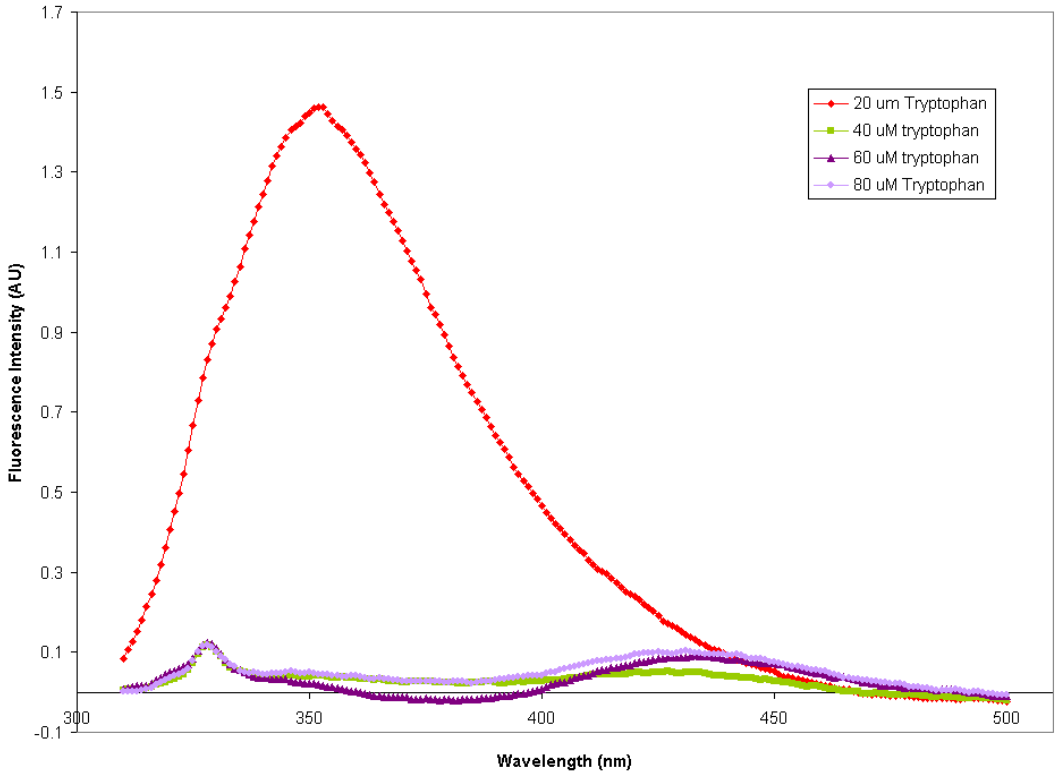

Figure 22. Fluorescence spectra of 80 nm gold nanoparticles titrated with various concentrations of tryptophan.

Figure 22 shows an increased intensity of the sample with 80 nm gold nanoparticles with only the 20 uM of tryptophan. The other samples containing 80 nm gold nanoparticles titrated with 40 uM, 60 uM, and 80 uM tryptophan have their intensity values quenched compared to tryptophan-only samples with respective concentrations. The intensity values increased for all other sizes of gold nanoparticles, but these 80 nm gold particles quenched completely with an increase in tryptophan concentration. This must indicate some interaction of energy transfer that quenches the fluorescence between large nanoparticles of gold and high tryptophan concentrations.

Table 10. Fluorescence intensity values of samples at 350 nm containing 10 nm, 20 nm, 40 nm and 80 nm sizes of gold nanoparticles titrated with varying concentrations of tryptophan.

Tryptophan conc (uM)	Tyrptophan Flu.intensity	AuNP 10 nm+Tryptophan Flu.intensity	AuNP 20 nm+Tryptophan Flu.intensity	AuNP 40 nm+Tryptophan Flu.intensity	AuNP 80 nm+Tryptophan Flu.intensity
20	0.72	1.8	0.74	0.78	1.5
40	1.71	2.1	1.6	1.8	0.11
60	2.3	2.7	2.3	2.5	0.13
80	3.4	3.5	3.0	3.1	0.14

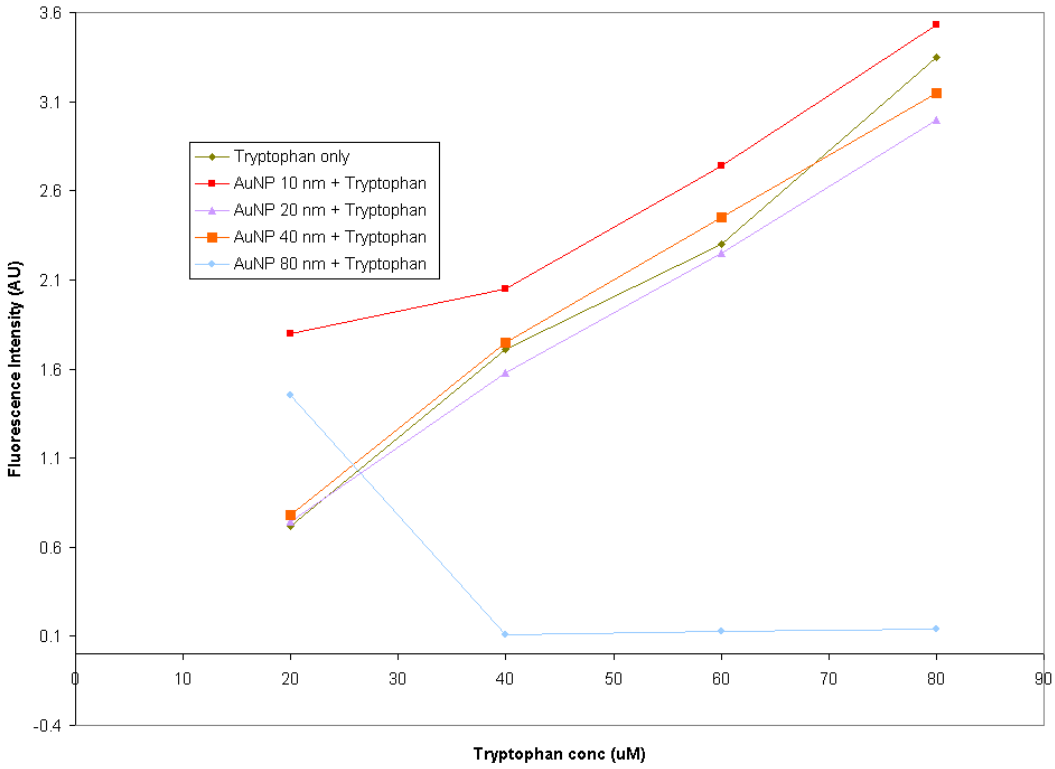

Figure 23. Fluorescence intensity values of samples at 350 nm containing 10 nm, 20 nm, 40 nm, and 80 nm sizes of gold nanoparticles titrated with varying concentrations of tryptophan.

Overall, the intensity values increased with an addition of gold nanoparticles to tryptophan. There is a gradual increase in intensity with increase in tryptophan concentration except for 80 nm gold samples. This enhancement in intensities may be due to the interaction of gold with a ultraviolet absorption band at about 320 nm with the tryptophan emission at 320 nm.[57]

3.5 Steady state fluorescence measurements of samples containing different sizes of silver/gold nanoparticles titrated with varying concentrations of phenylalanine.

Fluorescence intensities of samples containing different sizes of silver/gold nanoparticles that were titrated with varying concentrations of phenylalanine were analyzed using the spectrofluorometer with the samples being excited at 240 nm. The emission spectra ranging from 260 nm – 350 nm were collected. Table 11 shows the scheme used for these experiments.

Table 11. Titration scheme for silver/gold nanoparticles with varying concentrations of phenylalanine.

AgNP/AuNP (mL)	Phenylalanine (mL) of 113 (uM) conc	Distilled water (mL)
0.5	0.50	2.5
0.5	1.0	2.0
0.5	1.5	1.5
0.5	2.0	1.0

3.5.1 Steady state fluorescent measurements of samples containing 15 nm and 40 nm silver nanoparticles titrated with varying concentrations of phenylalanine.

Different sizes of silver nanoparticles with various concentrations of phenylalanine were analyzed using the intensities shown in Figures 24 to 27.

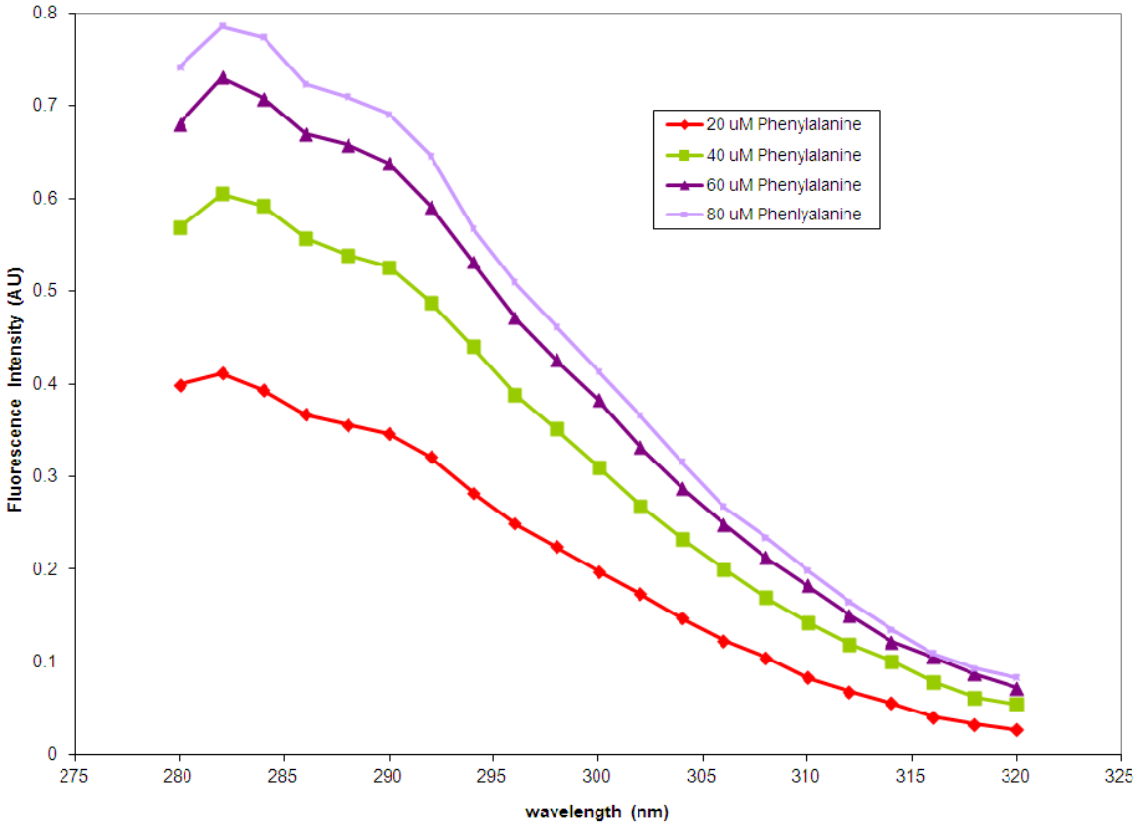

Figure 24. Fluorescence spectra of samples containing varying concentrations of phenylalanine.

Figure 24 shows increased fluorescence intensities with an increase in concentration of phenylalanine. The intensity verses concentration of these samples follows a linear function as in Beer's Law.

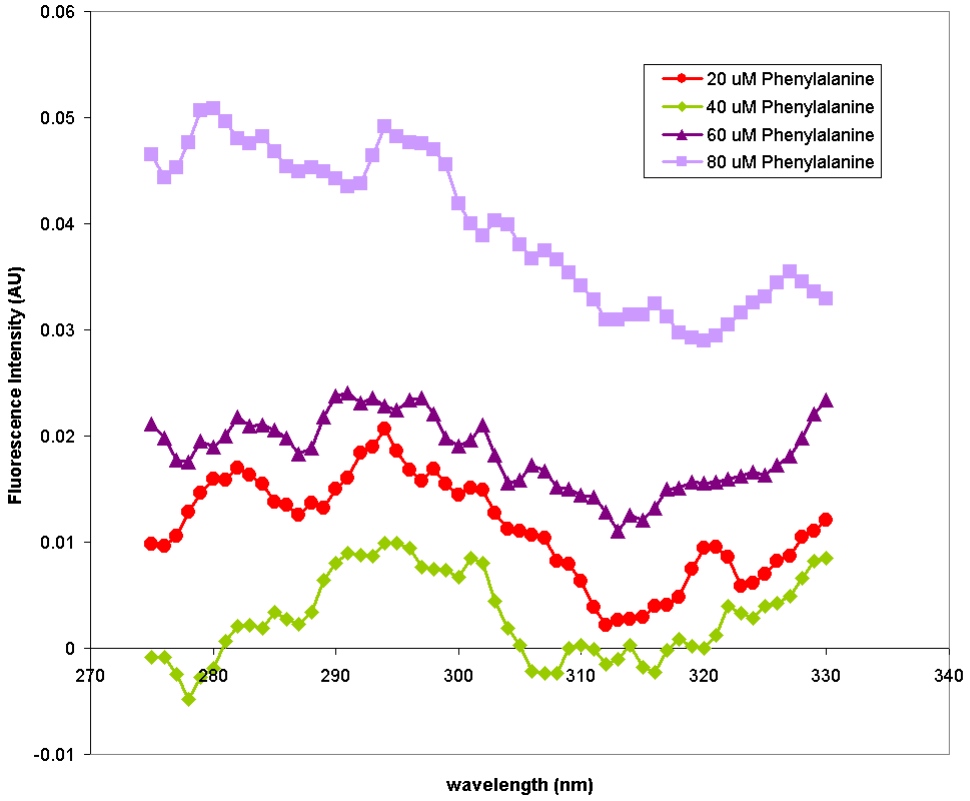

Figure 25. Fluorescence spectra of samples containing 15 nm silver nanoparticles titrated with various concentrations of phenylalanine.

Figure 25 shows fluorescence intensities with increase for several phenylalanine concentrations. The addition of 15 nm silver nanoparticles to the phenylalanine samples quenched the fluorescence.

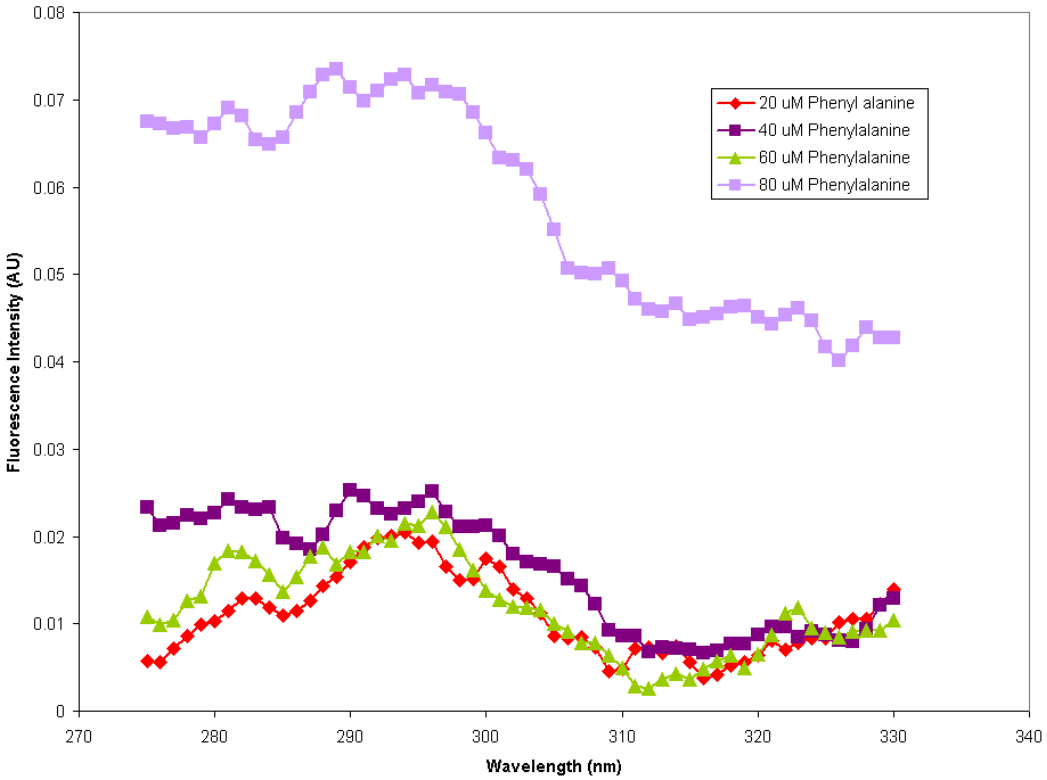

Figure 26. Fluorescence spectra of samples containing 40 nm silver nanoparticles titrated with various concentrations of 1 phenylalanine.

Figure 26 show fluorescence intensities for several phenylalanine concentrations. The addition of 40 nm silver nanoparticles to the phenylalanine samples quenched the intensities.

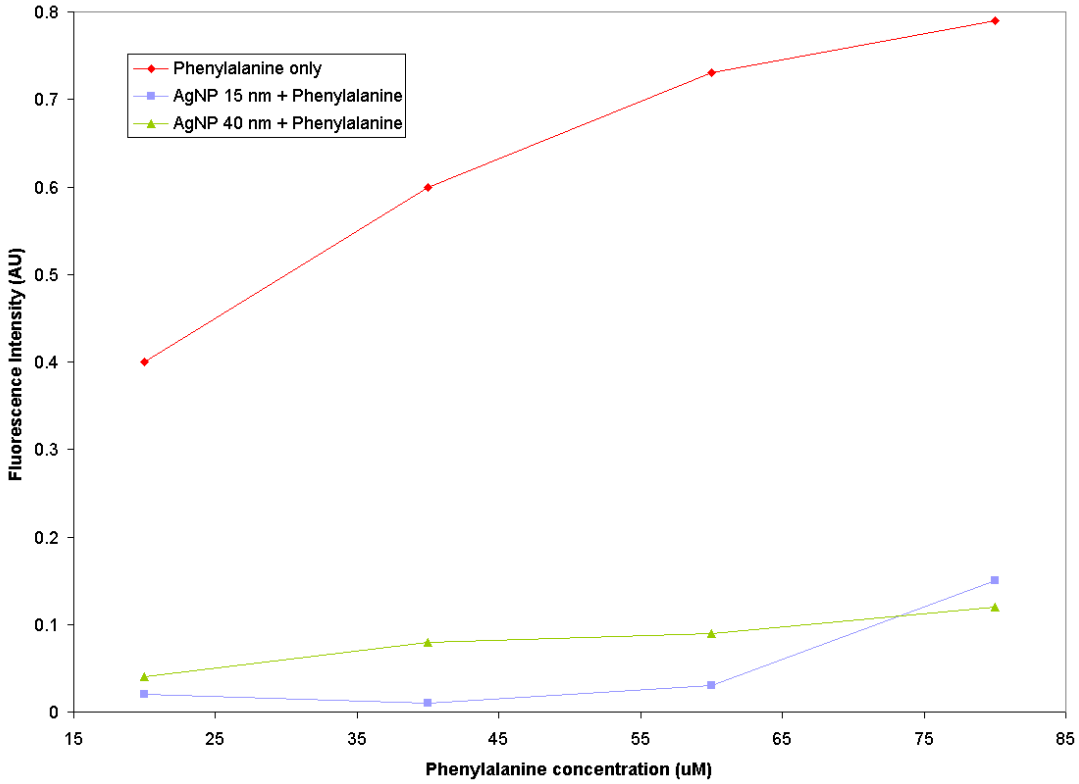

Figure 27. Fluorescence intensity values of samples at 285 nm containing 15 nm and 40 nm sizes of silver nanoparticles titrated with varying concentrations of phenylalanine.

Figure 27 shows the quenched fluorescence intensities when 15 nm and 40 nm silver nanoparticles were added to the phenylalanine samples. Smaller silver particles of size 15 nm greatly quenched, while 40 nm silver quenched to a lesser extent. There is a decrease in the 15 nm and 40 nm particle quenching, and the space between the curves is greater than experimental error. This quenching in the intensity is due to energy transfer from phenylalanine to silver nanoparticle. When a donor like tryptophan was placed in close vicinity of a conductive silver nanoparticle, resonance energy transfer takes place between tryptophan and silver, resulting in quenching of intensity. [56]

3.5.2 Steady state fluorescence measurements of samples containing 20 nm, 40 nm and 80 nm sizes of gold nanoparticles titrated with varying concentrations of phenylalanine.

Gold nanoparticles of sizes 20nm, 40 nm, and 80 nm were titrated with various concentrations of phenylalanine and then the fluorescence intensities were analyzed. Figures 28 to 31 show the results.

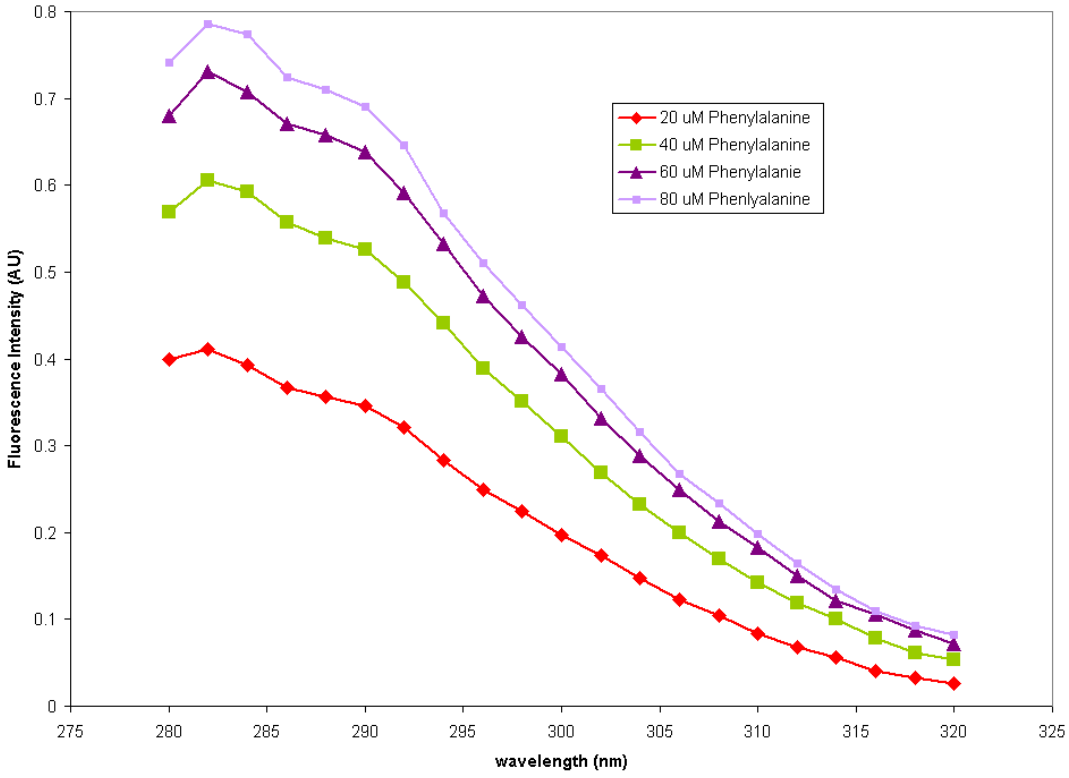

Figure 28. Fluorescence spectra of samples containing various concentration of Phenylalanine

Figure 28 show increased intensities with an increase in phenylalanine concentrations.

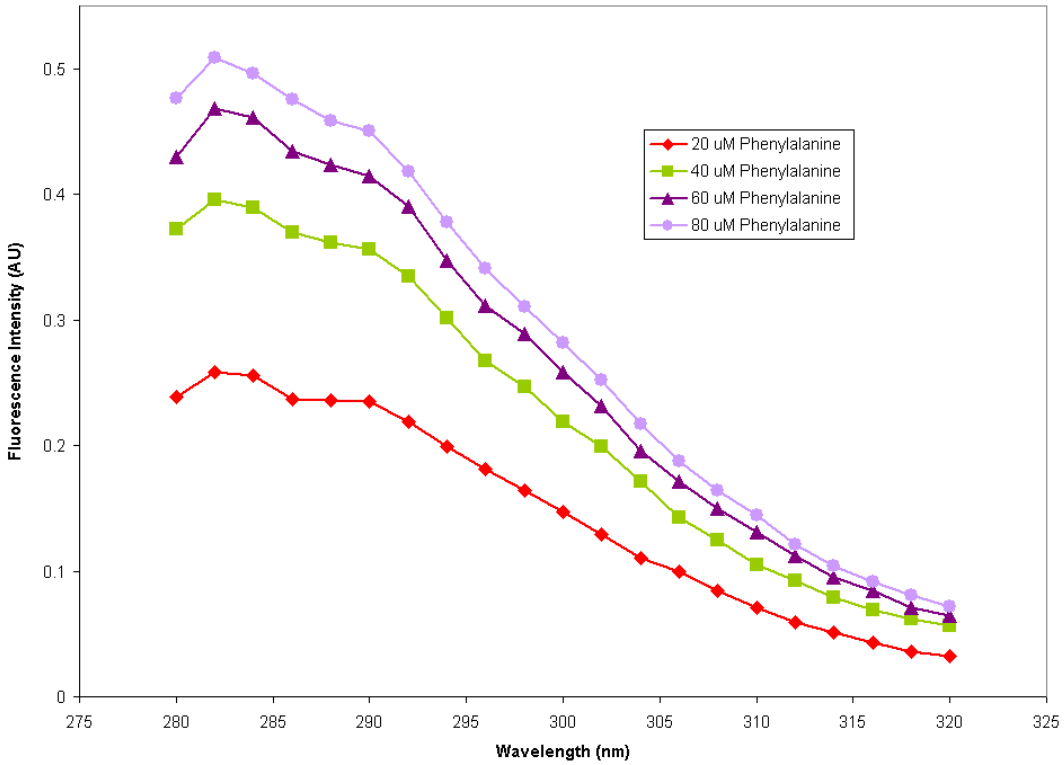

Figure 29. Fluorescence spectra of samples containing 20 nm gold nanoparticles titrated with various concentrations of phenylalanine.

Figure 29 also shows increased intensity with an increase in phenylalanine concentrations, but the addition of these 20 nm gold nanoparticles to the phenylalanine quenched the fluorescence intensity compared to the phenylalanine with no nanoparticles.

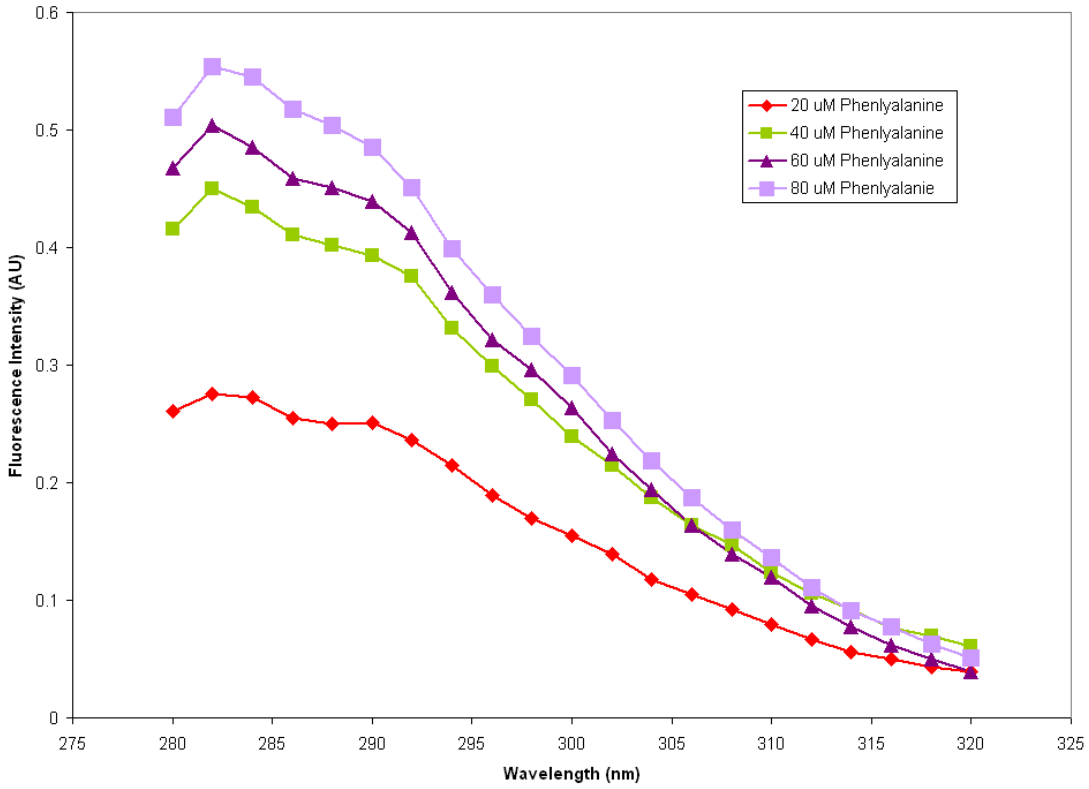

Figure 30. Fluorescence spectra of samples containing 40 nm gold nanoparticles titrated with various concentrations of phenylalanine.

Figure 30 shows that the addition of 40 nm gold nanoparticles to the phenylalanine quenched the fluorescence intensity. The 40 nm gold nanoparticles quenched less than 20 nm gold nanoparticle samples.

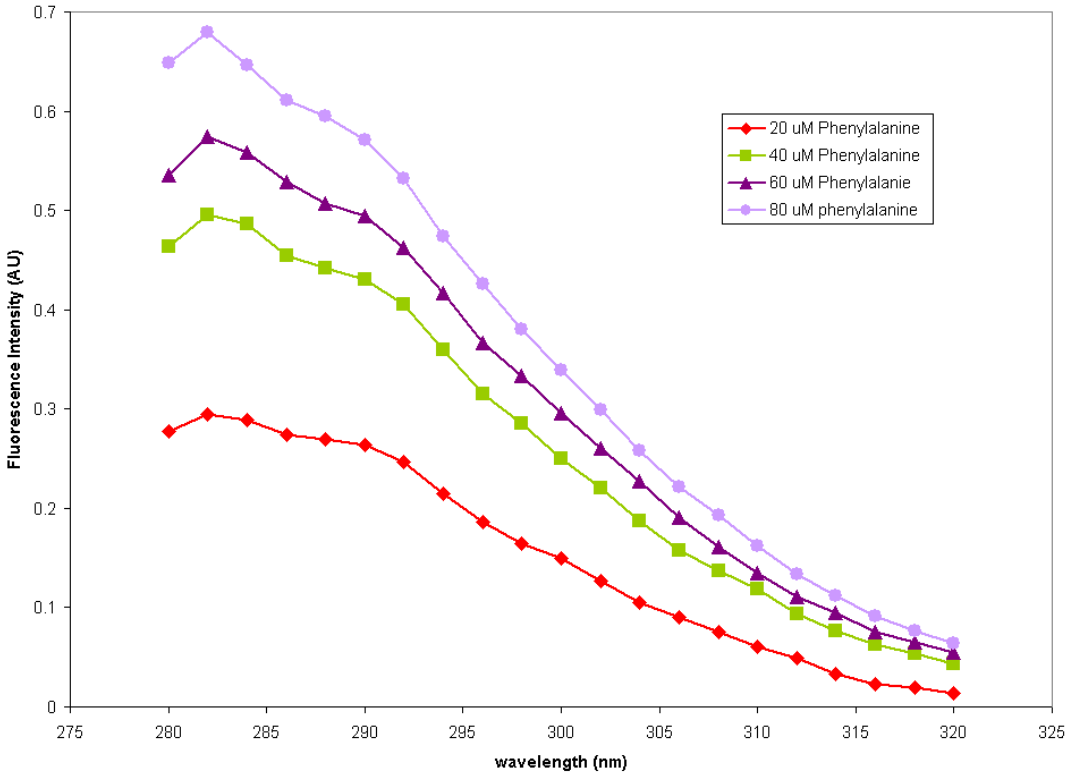

Figure 31. Fluorescence spectra of samples containing 80 nm gold nanoparticles titrated with various concentrations of phenylalanine.

Figure 31 shows increased intensities with an increase in phenylalanine concentrations, but similar to the other sizes, addition of these 80 nm gold nanoparticles to the phenylalanine samples quenched the intensity. The 80 nm gold nanoparticles quenched less than the 20 nm and 40 nm gold nanoparticle samples.

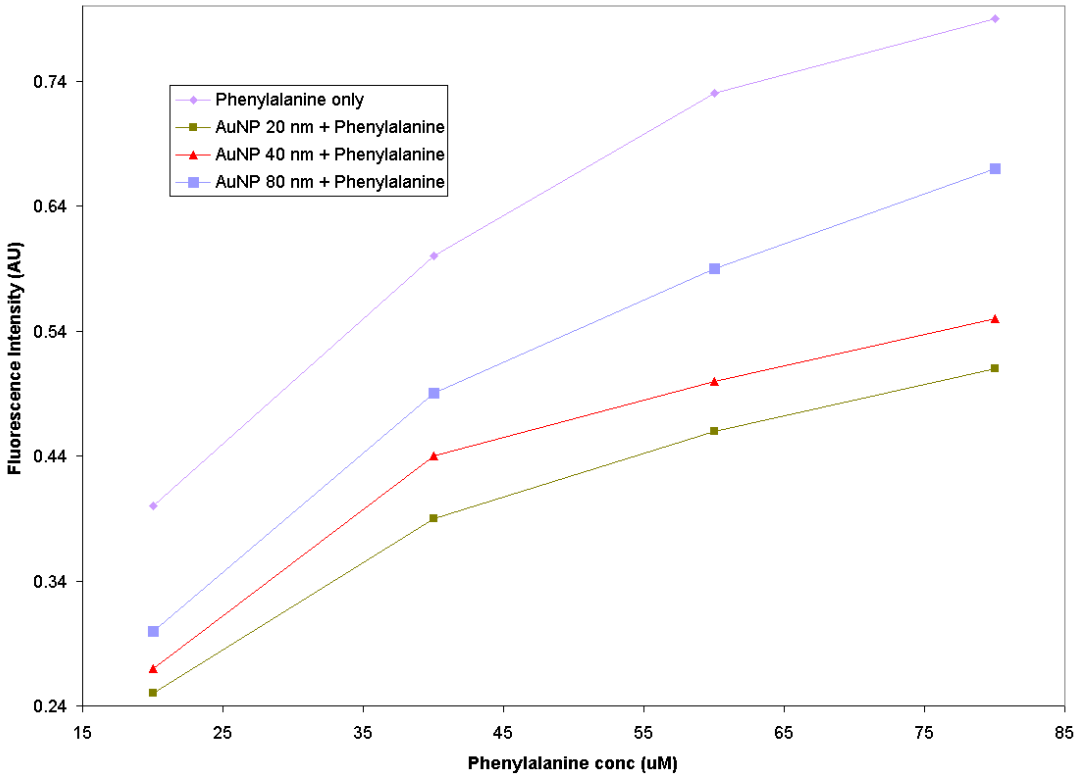

Figure 32. Fluorescence intensity values of samples at 285 nm containing 20 nm, 40 nm, and 80 nm sizes of gold nanoparticles titrated with varying concentrations of phenylalanine.

Figure 32 shows intensity values of different sizes of gold nanoparticles titrated with various phenylalanine concentrations. These results show the intensity values increased with an increase in phenylalanine concentration, but the addition of gold nanoparticles to phenylalanine samples quenched the fluorescence intensities. This quenching in intensity depends on the size of the gold nanoparticles. 20 nm gold nanoparticles quenched more than 40 and 80 nm gold nanoparticles. With a decrease in particle size, the relative surface area increases. This increased surface area can accommodate larger number of tryptophan molecules around the gold nanoparticles, making smaller particles efficient quenchers.[56]

CHAPTER 4

SUMMARY

Using three different methods we were able to synthesize various sizes (15 nm, 40 nm, 55 nm, and 80 nm) of silver colloids. The sizes of the nanoparticles were characterized by comparing the measured maximum absorbance wavelength values of the synthesized silver nanoparticles with the literature values.

The gold nanoparticles were synthesized by the reduction of $HAuCl_4$ by various concentrations of sodium citrate. The sizes of nanoparticles were characterized by comparing the measured maximum wavelength values of the synthesized gold nanoparticles with the literature values.

Different sizes of silver and gold nanoparticles were used to explore the size effect of these nanoparticles on the properties of fluorescents dyes like tris (2,2-bipyridyl) dichloro ruthenium(II) hexahydrate, tryptophan, and phenylalanine. The lifetime of samples containing different sizes of silver and gold nanoparticles with varying concentrations of ruthenium complex increased with an increase in the size of nanoparticles at constant ruthenium complex concentration. This increase in lifetime of the samples with smaller and larger silver and gold nanoparticles was only minimal, whereas the 40 nm and 50 nm silver nanoparticles and 10 nm gold nanoparticles show significant increases in their lifetime values. These longer lifetimes are due to the interactions of fluorophores with nanoparticles and surface energy transfer. In the presence of silver and gold nanoparticles, quenching of the fluorescence in the ruthenium complex and phenylalanine is observed. The binding of these nanoparticles to the above dyes have caused the

fluorescence to quench. This quenching was due to electron and energy transfer phenomena. It was observed that ruthenium and phenylalanine molecules exhibit various intensity profiles in the presence and absence of different sizes of silver and gold nanoparticles. The smaller nanoparticle sizes greatly quench the ruthenium complex and phenylalanine intensities, while the larger nanoparticles quench to a lesser extent. These lowered intensities show that nanoparticles were responsible for this quenching effect. These silver and gold nanoparticle surfaces induce strong quenching of fluorescence due to electromagnetic coupling between these metals and fluorophores.

The fluorescence rate of fluorophore is a function of the distance between the fluorophore and the nanoparticles. In general electron and energy transfer were the deactivation pathways for these excited fluorophores on the silver and gold nanoparticles. As all the sizes of the silver and gold nanoparticles used in the experiment were bigger than 5 nm, energy transfer dominates the quenching in this work. When donors like the ruthenium complex and phenylalanine were placed in the close vicinity of the conductive silver and gold nanoparticles, resonance energy transfer takes place between the donor and acceptor, leading to quenching in the intensities. As the size of silver and gold nanoparticles decreased, there was an increase in the relative amount of surface area. The increase in surface area can accommodate a larger number of ruthenium and phenylalanine molecules, making these smaller nanoparticles efficient quenchers.

On the other hand, the tryptophan on silver and gold nanoparticles showed a enhanced fluorescence, dependent on the size of the nanoparticles. This enhancement in intensities was due to resonance energy transfer and local electromagnetic field

enhancements of surface plasmon resonance in silver and gold nanoparticles. The distance between the nanoparticle and tryptophan plays an important role in influencing the emission intensities. This increase in emission intensities of tryptophan results from the enhancement effect of incoming and outgoing electric fields via coupling to the surface plasmon resonance in silver and gold nanoparticles. The observed enhancement of the fluorescence intensity from tryptophan in the presence of silver can be attributed to the electromagnetic field enhancement of silver nanoparticles, which was induced by the excited plasmons in the silver nanoparticles. The emission band of tryptophan produced, when excited at 280 nm overlaps with the surface plasmon resonance band of gold, nanoparticles ranging from 518 nm - 535 nm, which led to the enhanced intensity of tryptophan. The intensity of tryptophan increased with an increase in particle size from 20 nm to 60 nm, but was quenched in the case of 80 nm gold particles.

Finally, there was enhanced fluorescence with tryptophan and quenched fluorescence with the ruthenium complex and phenylalanine. Thus the observed fluorescence properties of tryptophan in silver and gold nanoparticle colloids make it a better candidate for the design of analytical tools applicable for labeling, biosensing, and bioimaging as compared to tris (2,2-bipyridyl) dichloro ruthenium(II) hexahydrate, and phenylalanine in silver and gold nanoparticle colloids. Thus this experiment generally supports earlier models and shows that more studies are needed that do a more quantitative analysis of the dependence of quenching and enhancement upon the properties of both the nanoparticle and fluorophore involved in the system.

References:

1. Xie, F.; Baker, M. S.; Goldys, E. M. "Enhanced Fluorescence Detection on Homogeneous Gold Colloid Self-Assembled Monolayer Substrates." *Chem. Mater*. **2008**, *20*, 1788-1797.
2. Bardhan, R.; Grady, N.K.; Cole, J. R.; Joshi, A.; Halas, N. J. Fluorescence Enhancement by Au nanostructures. *ACS Nano***. 2009**, *3(3)*, 744-752.
3. Walker, N. *J. Science*. **2002**, *296,* 557.
4. Kovar, J. L.; Simpson, M.A.; Schutz-Geschwender, A.; Olive, D.M. A Systematic Approach to the Development of Fluorescent Contrast Agents for Optical Imaging of Mouse Cancer Models. *Anal. Biochem*. **2007**, *367*, 1-12.
5. Weissleder, R. "A Clearer Vision For in vivo Imaging." *Nat. Biotechnol*. **2001**, *19*, 316- 317.
6. Lakowicz, J. R. Raiative Decay Engineering 5: Metal enhanced Fluorescence and Plasmon Emission. *Anal. Biochem*. **2005**, *337*, 171-194.
7. Drexhage, K. H. Progress in Optics. *J. Phys. Chem*. **1974**, 161-232.
8. Geddes, C. D.; Lakowicz, J. R. *J. Fluoersc*. **2002**, *12*, 121-129.
9. Matveeva, E.; Gryczynski, Z.; Malicka, J.; Gryczynski, I.; Lakowicz, J.R. *Anal. Biochem*. **2004**, *334*, 303-311.
10. Zhang, J.; Malicka, J.; Gryczynski, I.; Lakowicz, J. R. *J. Phys. Chem. B*. **2005**, *109,* 3157-3162.
11. Rossi, N. L.; Mirkin, C. A. *Chem. Rev*. **2005**, *105*, 1547-1562.
12. Shenhar, R.; Rotello, V. M. *Acc. Chem. Res***. 2003**, *36*, 549-561.
13. Katz, E.; Willner, I. *Angew. Chem. Int. Ed*. **2004**, *43*, 6042-6108.

14. Kerker, M. "The scattering of Light and other Electromagnetic Radiation". *Academic Press.New York*. **1969**.

15. El-Sayed, M. A. *Acc. Chem. Res*. **2004**, *37,* 326-333.

16. Hao, E.; Schatz, G.; Hupp, J. *J. Fluoresc*. **2004**, *14*, 331.

17. Wang, Y.; Herron, N. *J. Phys. Chem*. **95**, 525.

18. Kerker, M. *J. Colloid Interface. Sci*. **1985**, *105*,297.

19. Mie, G. *Ann. Phys*. **1908**, *25,* 329.

20. Alivisatos, A. P. *J. Phys. Chem*. **1996**, *100*, 13226.

21. Ahmadi, T. S.; Wang, Z. L.; Green, T. C.; El-Sayed, M. A. *Science*. **1996**, *272*, 1924.

22. Link, S.; El-Sayed, M. A. *J. Phys.Chem.B*. **1999**, *103*, 8410-8426.

23. Haynes, C. L.; Van, Duyne, R. P. *J. Phys. Chem. B*. **2001**, *105,* 5599-5611.

24. Aslan, K.; Huang, J.; Wilson, G. M.; Geddes, C. D. *J. Am. Chem. Soc*. **2006,** *128*, 4206.

25. Song, J. H.; Atay, T.; Shi, S.; Urabe, H.; Nurmikko, A.V. *Nano Lett*. **2005**, *5*, 1557.

26. Geddes, C .D.; Lakowicz, J. R . *J. Fluoresc*. **2002**, *12*, 121-129.

27. Lakowicz, J. R. *Anal. Biochem*. **2001**, *298,* 1-24.

28. Lokowicz, J. R.; Shen, Y.; Auria, S.D.; Malicka, J.F.; Gryczynski, Z.; Gryczynski, I. *Anal. Biochem*. **2002**, *301*, 261-277.

29. Gryczynski, I.; Malika, J.; Grynzynski, Z.; Geddes, C. D.; Lakowicz, J. R. *J. Fluoresc*. **2002**, *12*, 11-13.

30. Strickler, S. J.; Berg, R. A. *J. Chem. Phys*. **1962**, *37*, 814-822.

31. Sokolov, K.; Chumanov, G.; Cotton, T.M. *Anal. Chem*. **1998**, *70*, 3898-3905.

32. Selvan, S. T.; Hayakawa, T.; Nogami, M. *J. Phys. Chem. B*. **1999**, *103*, 7064-7067.

33. Mertens, H.; Biteen, J. S.; Atwater, H. A.; Polman, A. *Nano. Lett*. **2006**, *6*, 2622.

34. Duan, C.; Cui, H.; Zhang, Z.; Liu, B.; Guo, J.; Wang, W. *J. Phys .Chem. C*. **2007**, *111*, 4561.

35. Gersten, J. I.; Nitzan, A. *Surf. Sci*. **1985**, *158*, 165.

36. Kerker, M.; Blatchford, C. G. *Phys. Rev*. *B*. **1982**, *26*, 4082.

37. Aslan, K.; Lakowicz, J. R.; Mateeva. E.; Zhang, J.; Badugu, R.; Huang, J. *J. Fluoresc*. **2004**, *14*, 425.

38. Stoermer, R. L.; Keating, C. D. *J. Am. Chem. soc*. **2006**, 128, 13243.

39. Aslan, K.; Malyn, S. N.; Geddes, C. D. *J. Fluoresc*. **2007**, *17*, 7.

40. Frens, G. *Nat. Phys. Sci*. **1973**, *241*, 20-22.

41. Ray, K.; Badugu, R.; Lakowicz, J. R. *J. Phys. Chem. B*. **2006**, *22*, 8374-8378.

42. Fu, y.; Lakowicz, J. R. *Anal. Chem*. **2006**, *78*, 6238-6245.

43. Aslan, K.; Leonenko, A.; Lakowicz, J.r.; Geddes, C. D. *J . Fluoresc*. **2005**, *15*, 643-654.

44. Fu, Y.; Lakowicz. J. R. *J. Phys. Chem*. *B*. **2006**, *110*, 22557-22562.

45. Hines, M. A.; Guyot-Sionnest, P. *J. Phys. Chem*. **1996**, *100*, 468-471.

46. Dulkein, E.; Mortenni, A. C.; Niewdereichholz, T.; Klar, T. A.; Feldmann, J.; Levis, S. A.; Van Veggel, F. C. J. M.; Reihoudi, D. N.; Moller, M.; Gittins, D. I. *J. Phys. Rev. Lett***. 2002**, *89*, 203002.

47. Coghlan, D. R.; Mackintosh, J. A.; Karuso, P. *Org. Lett*. **2005**, *7*, 2401.

48. Solomon, S. D.; Bahadory, M.; Jeyarajasingam, A.V.; Rutkowsky, S. A; Boritz, C. *J. chem. edu*. **2007**, *84*, 322-325.

49. Cyrankiewicz, M.; Wybronowski, T.; Kruszewski, S. *J. Phys*. **2007**, *79.*

50. Patakfalvia, R.; De, K. "Synthesis and Intercalations of Silver Nanoparticles in Kaolinite/DMSCO Complexes". *Applied Clay Science*. **2004**, *25*, 149-159.

51. Saui, T. K.; Pal, A.; Jana, N. R.; wwang, Z. L.; Pal, T. "Size Controlled Synthesis of Gold Nanoparticles using Photochemically Prepared Seed Particles." *J. Nano. Res*. **2001**, *3,* 257-261.

52. http://en.wikipedia.org/wiki/Ultraviolet-visible_spectroscopy, 11/01/09, 5:00 pm.

53. http://en.wikipedia.org/wiki/Spectrofluorometer, 11/01/09, 6:45 pm.

54. http://en.wikipedia.org/wiki/Laser#Pulsed_operation, 11/02/09 10:30 am.

55. Suhov, N. L.; Ershov, N. B.; Mikhalko, V. K.; Gordeev, A.V. Absorption Spectra of Large Colloidal Silver Particles in Aqueous Solution. *Russian Chemical Bulletin*. **1997**, *46,* 197-199.

56. Ghosh, S. K.; Pal, A.; Kundu, S.; Nath, S. *Chem. Phys. Lett.* **2004**, *395*, 366-372.

57. Zhu, J.; Zhu, k.; Huang, L. Using Gold Colloid Nanoparticles to Modulate the Surface Enhanced Fluorescence of Rhodamine B. *Physical Letters. A* **2008**, *372*, 3283-3288.